UNIVERSITY OF TARTU
Faculty of Science and Technology
Institute of Technology

Eva Savulkina

Screening for novel components of intercellular network involved in growth and homeostasis of *Drosophila* wing imaginal disc

Bachelor's Thesis (12 ECTS)

Curriculum Science and Technology

Supervisor(s):
Professor, PhD, Osamu Shimmi

Tartu 2023

Screening for novel components of intercellular network involved in growth and homeostasis of *Drosophila* wing imaginal disc

Abstract:

The apicobasal polarity is an essential attribute of the epithelial tissue. The disruption of the apicobasal polarity is an essential attribute of the epithelial tissue. The disruption of polarity results in the loss of homeostasis and functionality of the tissue. The major apicobasal polarity determinant, tumour suppressor gene *scrib*, was found to be regulated by intercellular communications. When the conditional knockdown of *scrib* was introduced by patched-Gal4 driver, the progressive loss of polarity from the targeted cells to the neighbouring, healthy cells was observed. Recent studies further revealed that the interactions of Scrib with septate junctions components and the α-Catenin are crucial for sustaining intercellular communications. These findings suggest that a complex molecular network is involved in Scrib-mediated tissue homeostasis. To understand what molecules are needed to interact with Scrib, what mechanisms are utilized for mediating cell-cell communications for epithelial tissue development, and how they involve in the development of pathogenic processes, e.g., neoplasia formation, identification of the genes interacting with Scrib appears to be important.

In this thesis project, the *Drosophila melanogaster* wing imaginal disc was utilized as a model to explore potential gene candidates, interacting synergistically with *scrib* to maintain intercellular mechanisms during epithelial development. To achieve this goal, a two-step genetic screening was used by combining conditional RNAi knockdown of *scrib* and chromosome deficiency lines of the third chromosome in *Drosophila* in a sensitized background (heterozygous for candidate gens). The primary screening involved ten deficiency stocks that accounted for about 10% of the right arm of the third chromosome. Subsequently, a secondary screening was performed to narrow down the locus of deficiency by employing multiple deficiency lines that overlap with the candidate deficiency line from the primary screening. The results provide one strong deficiency line candidate, composed of 10 coding genes, that may have synergy with *scrib*.

Keywords:

scribble, *Drosophila*, deficiency lines, apicobasal polarity, RNAi, wing imaginal disc

CERCS: B350 Developmental biology, growth (animal), ontogeny, embryology

Äädikakärbse diivadiski kasvu ja homöostaasiga seotud uute rakkudevaheliste molekulaarsete komponentide sõeluuring

Lühikokkuvõte:

Apikobasaalne (AB) polarisatsioon on epiteliaalsetele rakkudele omane oluline tunnus. Muutused AB polarisatsioonis võivad viia kudede homöostaasi ja funktsiooni kadumiseni. Üks peamisi AB polarisatsiooni eest vastutavaid molekulaarseid determinante on tuumor-supressor valk scribble, mis on osaline ka rakkudevahelisel kommunikatsioonil. Kui äädikakärbse tiivadiskis konditsionaalselt osades rakkudes scribble alla suruda patched-Gal4 draiveri poolt, siis indutseerib see neid ümbritsevates normaalsetes rakkudes progresseeruva AB polarisatsiooni kadumise. Hiljuti on leitud, et scribble interakteerub rakkudevaheliste liiduste (*septate junctions*) komponentidega ja α-kateniiniga, mis viitab sellele, et epiteliaalsete kudede homöostaasi säilimiseks on vajalik keerukate molekulaarsete võrgustike olemasolu. Millised molekulaarsed faktorid interakteeruvad veel scribble`ga ja millised mehhanismid vahendavad rakk-rakk kommunikatsiooni epiteliaalsete kudede normaalseks toimimiseks ning millist rolli mängivad need võimalike patogeneetiliste (nt kantserogenees) protsesside kujunemisel vajavad veel selgitamist.

Antud bakalaureusetöös kasutati äädikakärbse (*Drosophila melanogaster*) arenevat tiivadiski kui mudelit, et välja selgitada millised geenid interakteeruvad sünergistlikult scribble`ga, et säilitada epiteelirakkude omavaheline kommunikatsioon ja AB polarisatsioon. Eesmärgi täitmiseks kasutati kahe-etapilist geneetilist sõeluuringut, kus kombineeriti konditsionaalset *scrib*RNAi ja 3. kromosoomi defitsiitseid kärbseliine sensibiliseeritud taustal (uuritavate kandidaatgeenide suhtes heterosügootne). Esmasel (primaarsel) geneetilisel sõeluuringul kasutatud kaheksa erinevat 3. kromosoomi defitsiitset liini moodustab kokku 10% 3. kromosoomi paremast õlast. Järgnevalt teostati sekundaarne sõeluuring, mille käigus sõeluti välja üks 3. kromosoomi defitsiitse-liini kandidaat, kus defitsiitne piirkond koosnes10 kodeerivast geenist, millel võib olla sünergia *scrib*bl`ga.

Võtmesõnad:

scribble, äädikakärbes, defitsiitsed liinid, apikobasaalne polaarsus, tiiva imaginaaldisk,, RNAi

CERCS: B350 Arengubioloogia, kasv (loom), ontogenees, embrüoloogia

TABLE OF CONTENTS

TERMS, ABBREVIATIONS AND NOTATIONS

GFP – green fluorescent protein

scrib **-** *scribble*

Gal80^{TS} – Temperature-sensitive Gal80

Crb –Çrumbs

Dlg – Discs-large

Lgl – Lethal giant larvae

PDZ – postsynaptic density-95/Disc-large/ZO-1

LRR – leucine rich repeats

Hpo – Hippo pathway

Wts – Warts

Yki – Yorkie

RNAi – RNA interference

A/P – Anterior/Posterior

UAS – Upstream Activating Sequence

ABP – Apico-basal polarity

D-V – Dorsal-Ventral

TP – Thoracic imaginal disc primordia

Dll – Distal-less

Ex-LacZ – Expanded-lacZ

DP – disc proper

aPKC – atypical protein kinase C

AJs – Adherens Junctions

SJs – Septate Junctions

INTRODUCTION

Apicobasal polarity (ABP), a defining property of epithelial tissue, is crucial for maintaining tissue homeostasis. It has been observed that ABP is evolutionarily conserved across many species. Hence, the loss of polarity leads to tissue dysfunction in invertebrates and vertebrates (Gibson & Perrimon, 2003). The three main protein complexes determining the apicobasal polarity were recognised, including Crumbs, Par and Scribble (*scrib*) complexes. Scrib module comprise *scrib*, Dlg and Lgl proteins (Macara, 2004; Bonello & Peifer, 2019). Through antagonising interactions between these apical and basal modules, the proteins are restricted to localize at the opposing complex (Campanale *et al*., 2017). Scrib, as a key apicobasal polarity determinant, was also confirmed to be a tumour suppressor gene (Carmena, 2020). Within the wing imaginal disc epithelium, cells deficient for *scrib*, tend to overproliferate and form neoplastic masses. However, to keep overall tissue homeostasis, small clusters of the mutants are often eliminated by the neighbouring healthy cells (reviewed in Bowling *et al*., 2019). In contrast, if the oncogenic cells have mutations to evade their removal, these cells can influence surrounding cells, resulting in tissue disorganisation (C. Chen *et al*., 2012). Recent findings indicate that conditional knockdown of *scrib* within the *patched* region, which located within the stripe of cells on the A/P domains in wing disc, leads to the polarity determinant loss not only in the target region but also in the surrounding healthy cells prior to the disorganisation of tissue architecture. This reveals the role of cellular communications in the progressive restoration or loss of apicobasal polarity in the tissue and, in epithelial homeostasis and growth (Gui *et al*., 2021). It was discovered that Scrib sustains tissue homeostasis through cell-to-cell communication by interacting with the septate junction complex and α-Catenin. These findings incite the complex molecular network, involved in tissue homeostasis. However, the deep understanding of the mechanism and the specific genes that interact with Scrib, altering tumour progression through cell-to-cell interactions, remain to be investigated (Huang *et al*., 2023).

In this study, the UAS-GAL4/GAL80 system with *scrib* RNAi knockdown was utilized to carry out a two-step screening experiment for identifying novel candidate genes, interacting with *scrib*. Firstly, different deficiency lines of the third chromosome right arm under the *scrib* RNAi were screened to detect the possible gene candidates. After the primary screening, one strong deficiency line candidate with a wide gene region was identified. Secondly, to narrow down the number of genes, the screening of deficiency lines, genetically overlapping with the primary candidate was performed. Since the secondary screening outcome

supported the primary screening results, one potential gene region with 10 genes was found to have interactions with *scrib* in apicobasal polarity maintenance.

1 LITERATURE REVIEW

1.1 *Drosophila melanogaster* as a model organism in biological research

Drosophila melanogaster, fruit fly, is a small insect, around 3 mm long. *Drosophila melanogaster* has been implemented as a versatile model organism in various fields of biology, including genetics, developmental biology, and biomedicine (Tolwinski, 2017). There are various advantages to the fly model, among them the homology of *Drosophila*'s genome to the human of about 60%, and about 75% of the genes known to be responsible for human diseases have homologs in fruit flies. Apart from that, flies have a short life cycle, and maintenance is affordable and easy (reviewed in Mirzoyan *et al*., 2019).

Fruit fly undergoes complete metamorphosis in a relatively short time, which includes four main stages: embryonic, larval, pupal, and adult fly stages (Perveen, 2018, pp. 6–7) (Figure 1). After fertilisation, embryogenesis occurs at 25°C for 21-24 hours (Jennings, 2011). The subsequent larval stage can be divided into three stages (first, second, and third instar larval stages), which last around five days. Larvae use the food source to grow and store fats and sugars to sustain through metamorphosis in the following pupal stage (Allocca *et al*., 2018). In the final third instar stage, larvae leave the food substrate to pupate. Throughout the larvae stages, the exoskeleton is continuously shed in the moulting process, which is facilitated by several growth hormones (reviewed in Edgar, 2006). In addition, in holometabolous insects, the organs of the adult form are not developed until the completion of metamorphosis (Shingleton, 2010b).

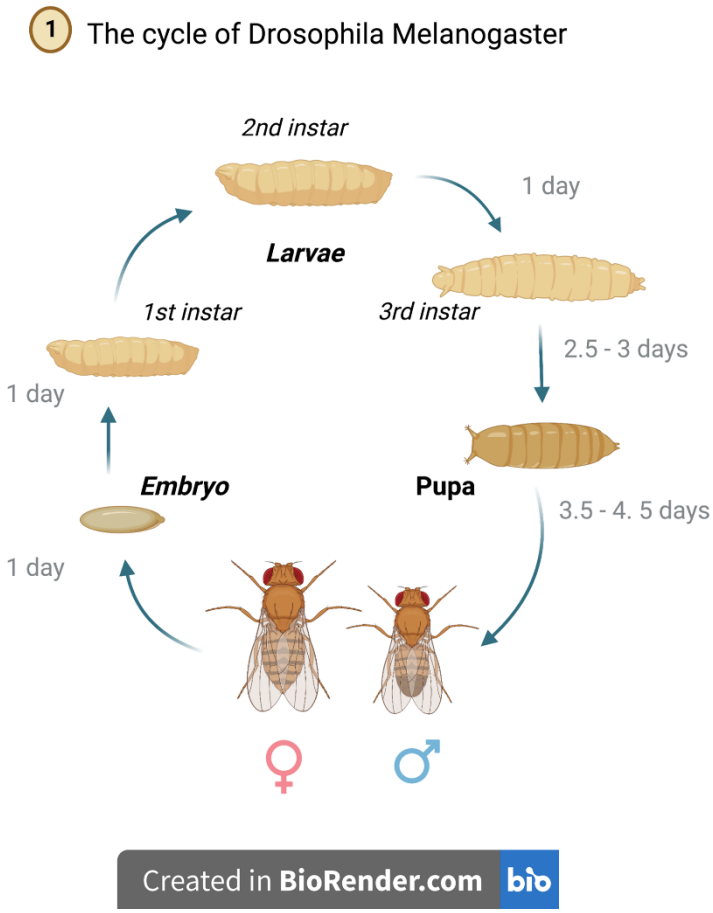

Figure 1. The life cycle of *D. melanogaster*. The *Drosophila* life cycle includes 4 stages, as follows: embryonic stage, larval stage, pupal stage, and adult stage. The following time points are valid in 25°C conditions.

Firstly, the progenitor structures, imaginal discs, are formed, each corresponding to a specific adult organ. In essence, imaginal discs are tissues of diploid cells of the undifferentiated epithelium. Each disc possesses unique characteristics, including its size, shape, histology, and patterning fate map (Ostalé *et al*., 2018). When metamorphosis occurs, imaginal discs differentiate and evaginate to form adult organs. Upon completion of the transformation, adult fly hatches (Shingleton, 2010c).

The implementation of *Drosophila melanogaster* as a model organism has led to numerous significant discoveries in the field of biomedicine. Thomas Hunt Morgan improved the inheritance theory introduced by G. Mendel by employing fruit flies. The scientist utilized flies to do breeding analysis and subsequently identify the inheritance patterns of the white-eye mutation. While conducting the test crosses between red-eyed and white-eyed flies, the researchers observed sex-linked heredity of the trait. Even before it was established that DNA

is a genetic material of the organism, Morgan had defined genes and proposed that chromosomes contained genes within them (reviewed in Benson, 2001). Morgan received the Nobel Prize in Physiology or Medicine in 1933 for his research concerning the involvement of chromosomes in heredity. One of his students, Hermann Muller, used *Drosophila melanogaster* to perform experiments on the influence of X-rays on the mutation rate of the organism. He discovered a strong correlation between irradiation and the production of mutations, which led to the realisation that genetic defects in the offspring are the consequences of parental radiation exposure. In addition, Muller was honoured with the Nobel Prize in Physiology or Medicine in 1946 for his findings in mutagenesis by means of X-ray irradiation (Jennings, 2011). Thus, for more than a century, *Drosophila* has served as an efficient model organism used to investigate biological mechanisms, genetics, and inheritance.

1.1.1 Genetic tools for tissue-specific regulation of gene expression in *Drosophila*

Since the first discoveries, many genetic tools have been invented and employed in the fruit fly model, enabling the regulation of transcription for particular genes in a tissue-specific manner or a whole organism. These methods can be of great use since researchers can gain valuable insights into the formation and regulation of the imaginal discs and, consequently, into fundamental processes influencing tissue development (reviewed in Beira & Paro, 2016). One of the most used genetic manipulation techniques in *Drosophila* is the UAS/GAL4 system (Duffy, 2002; Figure 2a). In essence, this method is based on a binary expression system that allows the creation of targeted activation of genes of interest in a particular group of cells (Brand & Perrimon, 1993). Furthermore, the system can be enhanced with $Gal80^{TS}$ to achieve better temporal control and RNA interference (RNAi) to accomplish spatial regulation over gene knockdown in fly tissue or imaginal discs (Figure 2b), (Blake *et al*., 2017).

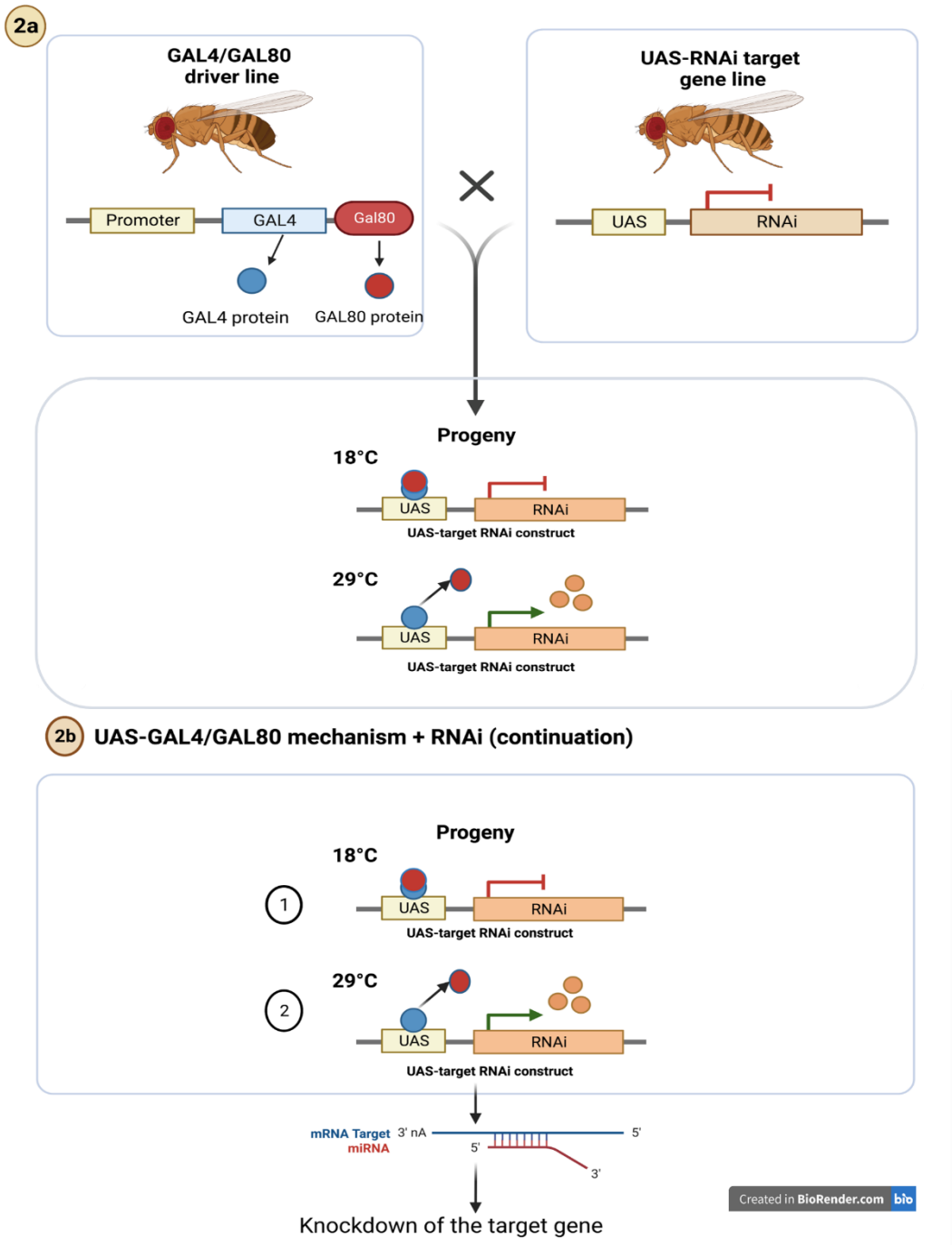

Figure 2. The mechanism of UAS/GAL4/ Gal80^{TS} with RNAi in the *D. melanogaster* model organism. (A) The UAS/GAL4/ GAL80^{TS} cross setup. In the following progeny, GAL4 activates transcription of genes under Upstream Activating Sequence (UAS). GAL 80^{TS} binds to GAL4 at 18° and inhibits the activity of GAL4. At 29°C, GAL 80^{TS} is inactive and degrade; GAL4 induces the expression of gene. **(B) RNAi mechanism.** At 29°C, the dsRNA is trans*crib*ed by GAL4 and are targeted to degrade the transcript of the gene of interest, leading to knockdown of the target gene.

In fruit flies, the GAL4 gene is placed under a tissue-specific promoter to achieve tissue-specificity (Figure 2a). Moreover, the $GAL80^{TS}$ gene could be added to the system to achieve better control of the conditional expression. Binding of $GAL80^{TS}$ gene to the GAL4, represses the latter. (Duffy, 2002) Its expression is temperature sensitive. At 18°C, $GAL80^{TS}$ acts as a repressor of GAL4, stopping its recruitment of transcriptional machinery. However, at 29°C, it is inactive and degraded. (Barwell et al., 2017) Therefore, the implementation of the GAL4/UAS+$GAL80^{TS}$ system results in the of expression based on tissue type and temperature.

RNAi in *D. melanogaster* can be achieved with a sequence of hairpin dsRNA complementary to the endogenous gene of interest and can be introduced into the chromosome under the control of the GAL4/UAS system (Heigwer et al., 2018). It results in gene silencing in the specific tissue and with the addition of $Gal80^{TS}$ – incorporation of temperature sensitivity in the system (Figure 2b).

Additionally, the imaginal discs as experimental model systems are beneficial since these structures are sensitive to experimental manipulations throughout development. At the same time, the growth and differentiation proceed at a clock-like precision cell division. Besides, the morphology of the imaginal discs facilitates the screening experiments. Imaginal discs are transparent, simplified models shaped like flattened sacs, and these properties ease the dissection and staining, essential methods in visualising the protein of interest (Ostalé et al., 2018).

Ultimately, *Drosophila melanogaster* is a favoured model organism in biomedical research. Employing fruit flies is an efficient way to study disease processes, given the homology between insects and mammals, the variety of genetic tools, and the rapid life cycle. By utilising the UAS/GAL4/$GAL80^{TS}$ system in the imaginal disc, the development of the epithelial tissue with visualised protein of interest can be examined.

1.2 Genome of *Drosophila melanogaster*

The organisation of the fruit fly's genome makes it practical for genetic manipulations. *Drosophila melanogaster*'s karyotype is comprised of four chromosomes. They include the X and Y sex chromosomes, the autosomal chromosomes 2 and 3, and a small chromosome 4. Latter contains no more than 100 genes and is known as the "dot chromosome" (Llorens-Giralt *et al*., 2021). Both female and male flies have two autosomal second, third, and fourth chromosomes (Kaufman, 2017). The sex determination in *Drosophila* relies on the dosage of the X chromosome (X: A ratio), the ratio of the number of X chromosomes to the number of sets of autosomes. The genome of *D. melanogaster* contains 17,728 genes and based on the latest genome assembly, the number of protein-coding genes reaches 13,920 (Hales *et al*., 2015b). The estimated entire *Drosophila* genome size is ∼180 Mb, where ∼120 Mb accounts for euchromatin (reviewed in Adams *et al*., 2000). Nowadays, researchers can utilise the database "FlyBase", the primary repository of genetic and molecular data for the *Drosophila melanogaster*. It is beneficial for collecting information about specific genomic locations, genetic interactions, and mutant phenotypes (FlyBase, n.d.).

Thus, the combination of the genome structure of *Drosophila melanogaster* with genetic tools available for the model organism provides an effective model system for conducting genetic screenings and mutation studies.

1.3 Wing imaginal disc

Drosophila's imaginal discs represent a convenient model system for exploring the functional role of genes in epithelial development and organ morphogenesis. The extensive growth of the wing disc, the largest among the discs in *Drosophila* (Porter & Rivers, 1975, p.78), has made it a valuable tool for investigating molecular mechanisms and identifying genes that have essential roles in controlling tissue growth and patterning (Dye *et al*., 2017). The study of the wing disc holds considerable significance since about 90% of human cancers are of epithelial origin (Mirzoyan *et al*., 2019). The wing disc's flat morphology, with most cells arranged in a single epithelial layer, has made it easier to use imaging-based techniques, thus providing a versatile model system (Aldaz *et al*., 2010). An in-depth understanding of the factors contributing to overproliferation and subsequent tumorigenesis can be achieved through the analysis of the wing disc development stages, its formation into an adult wing, and the molecular pathways that regulate its progression.

Initially, the wing disc is given rise to during embryogenesis from a cluster of ~30 primordial cells, which further invaginate to form a flattened sac-like structure (Everetts *et al*., 2021). The primordial cells reside in the lateral epidermis of T2 around embryonic stages 11–13 (Requena *et al*., 2017). Primordial cells are identified based on morphology, along with specific molecular markers (e.g., transcription factors) that are expressed within cell populations (Figure 3A). The development of wing discs is tightly linked to the patterning process, which includes the division of the domains of cells into compartments, which share a common ancestry and adhesive properties. Compartments are distinct units controlled by the selector genes. Signalling between the compartments is maintained by the anterior-posterior (A/P) and dorsal-ventral (D-V) organisers. Thoracic imaginal disc primordia (TP), responsible for developing both leg and wing disc, are identified by the expression of the Distal-less (Dll) transcription factor at the embryonic stage 11 (reviewed in Tripathi & Irvine, 2022). Further dorsal migration of the wing disc primordia (~25-30 cells) physically separates populations of cells responsible for developing the wing and leg discs (Requena *et al*., 2017).

During larvae stages, the wing disc proliferates rapidly, forming a matured disc comprising approximately 35,000 cells, which possess different cell fates in the distinct regions, shaping the precursor structure (reviewed in Tripathi & Irvine, 2022). The wing imaginal disc is divided into three central regions based on the adult wing structures they produce: the pouch, hinge, and notum (Figure 3B) (reviewed in Klein, 2001).

3 Wing imaginal disc development and patterning

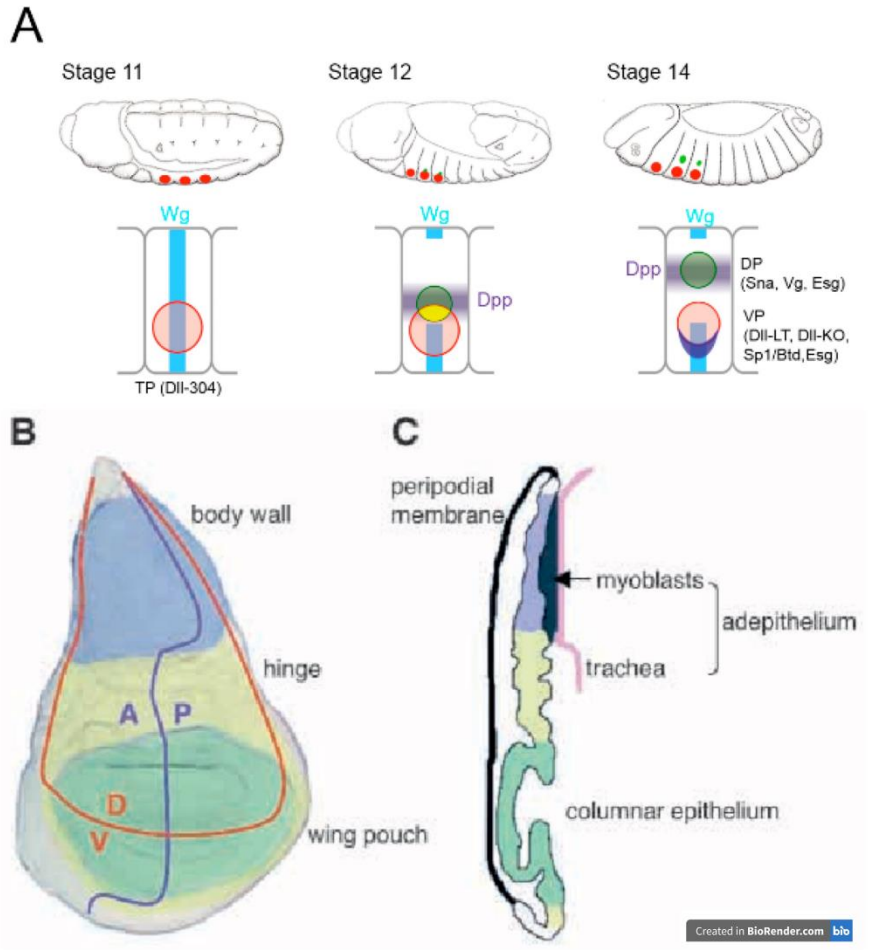

Figure 3. Wing imaginal disc development and patterning. A) Thoracic primordial cells location in the embryonic stages (11-14) (Ruiz-Losada et al., 2018). At stage 11: Dll expression (red circle) activates by Wg and repressed dorsally and ventrally by the Dpp and EGFR pathways. At stage 12: Doc is induced by Dpp and inhibits Wg in the lateral ectoderm. At stage 14: the wing and haltere are fully separated. **B)** The regions of wing imaginal disc: notum (body wall), hinge and wing pouch. The signalling between compartments is divided by the organisers, - anterior-posterior (A/P) and dorsal-ventral (D/V). C) Cross section showing the peripodial membrane and the disc proper (columnar epithelium).

In the early stages, first and second instar larval stages, the wing disc is shaped as a flat sac of cuboidal epithelial cells, with the apical sides toward the lumen. While the disc grows, the cellular morphology begins to vary, producing two opposing layers: a peripodial epithelium (PE) and disc proper (DP). The first one is characterised by flattened cells, forming a thin squamous epithelium. In contrast, DP is formed as a columnar epithelium due to their

apico-basal elongation in the increased population. By the late third instar, the columnar cells are tightly compacted and elongated, particularly in the pouch region, which develops in the wing blade. These changes in cell shape and organisation in the pouch region can lead to a pseudostratified epithelium with nuclei at different heights The folds between hinge-notum (top), hinge–hinge (middle), and hinge–pouch (bottom) is (Figure 3C) generated (reviewed in Tripathi & Irvine, 2022).

Subsequently, at the pupal stage, the wing disc undergoes morphogenesis and, after further differentiation, forms an adult wing and notum. The transformation is achieved through eversion, leading firstly to the formation of a rudimentary wing and, afterwards, to the formation of a three-dimensional wing of dorsal and ventral epithelial cells (Gui *et al*., 2019). Hence, the unique properties of the wing disc, including its structure (a monolayer of the columnar epithelium) and its rapid growth rate during development, compose a promising model system to research excessive proliferation and cancer development.

1.4 Apicobasal polarity of epithelial cells in wing imaginal discs

Cell polarity is defined by the asymmetrical distribution of cell components and may occur in distinct forms. Cell polarity formation facilitates the distinct shaping of the cell adapted for its specific function. Cell polarity mechanisms govern the correct development of the organisms, including asymmetric cell divisions essential for self-renewal and differentiation processes (Lee & Vasioukhin, 2008). The cell polarisation process has been extensively studied in many organisms and appears to be evolutionarily conserved (Drubin & Nelson, 1996).

The coordinated organisation of epithelial cells is essential for several developmental processes, such as the establishment of barriers and the regulation of tissue architecture. In order to maintain proper functionality, epithelial cells typically exhibit apicobasal polarity (ABP) along the apical-basal axis. As a result, the distinct sub-compartments are organised along the axis and specific cellular functions are vectorised to the cell poles (reviewed in Thompson, 2013). In contrast, loss of ABP leads to dysfunction in a tissue and absence of homeostasis leading to neoplasia (Bilder, 2004; Igaki *et al*., 2006).

1.4.1 Apicobasal polarity complexes

Within the wing imaginal disc, three major conserved protein complexes controlling the ABP were identified, namely, Par, Crumbs, and Scribble (Figure 4). The complexes are localised in apical (Crumbs and Par) and basolateral domains (scribble) (Macara, 2004; Bonello & Peifer, 2019). The Par complex is composed of Par3, Par6, and atypical protein kinase C (aPKC). The Crumbs complex includes several components: the integral membrane protein, Crumbs (Crb), Stardust, Patj and Lin7. The basolateral Scribble complex is composed of the Scribble (*scrib*),

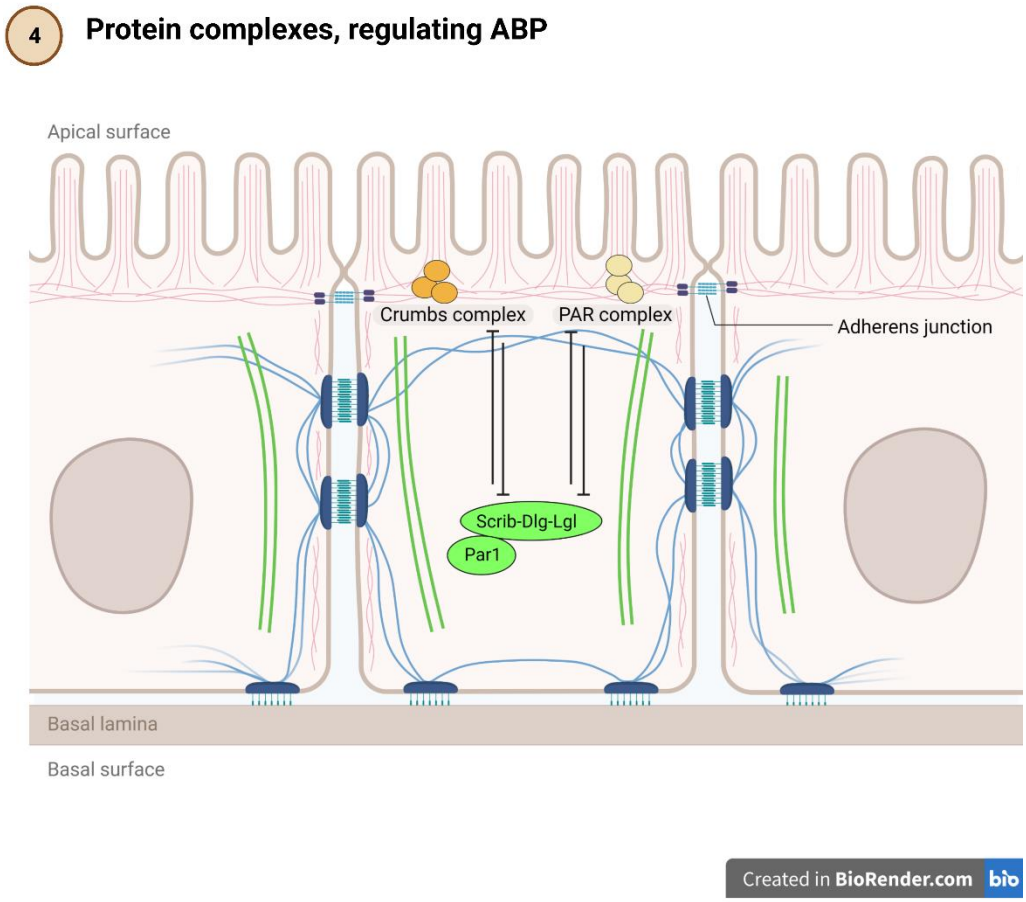

Figure 4. Protein complexes, regulating ABP. Three major complexes: Crumbs, Par, *scrib*, - composing the apical and basolateral complexes. Apical (Crumbs and Par) and Basolateral (*scrib*) complexes antagonise each other, to prevent the disruption of polarity.

Discs Large (Dlg) and Lethal Giant Larva (Lgl) compartments (reviewed in Riga *et al*., 2020; Campanale *et al*., 2017; Assémat *et al*., 2008). The apicobasal determinants in the same complex are interdependent on each other. The loss of one component will lead to the disruption of the whole complex. Conversely, determinants from distinct complexes show antagonistic interactions (Campanale *et al*., 2017). The Par and Crumbs compartments restrict

apical localization of basolateral polarity proteins, whereas the basolateral Scrib module acts in parallel to prevent basolateral localization of apical and junctional proteins. For instance, the Scribble module is known to antagonise apical Crumbs to localise basolaterally. aPKC phosphorylates PAR-1, Par3, and Lgl to exclude them from the apical domain. Therefore, the dysfunction of one sub-compartment localisation results in expansion or elimination of the other complexes, leading to the complete loss of ABP (Huang *et al*., 2023).

1.4.2 Epithelial cell junctions

Essential structures in maintaining ABP are cell-to-cell physical connections through particular junctions. One junction type is adherens junctions (AJs) (Figure 4), which are connected to the actin cytoskeleton, regulating apical cell shape, and facilitating cell-cell adhesion (reviewed in Tepass & Harris, 2007). They are composed of E-Cadherin (DE-Cadherin), linked to α-, β-, and p120-Catenins. E-Cadherin couples intercellular adhesion to the cytoskeleton via β-catenin (β-cat) and α-catenin (α-cat) (Rübsam *et al*., 2017). Apart from AJs, Septate Junctions (SJs), consisting of a large multi-protein complex, are located below the AJs at the boundary of apical and basal compartments. SJs are providing structural strength and a barrier to intercellular solutes diffusion (Baumgartner *et al*., 1996; Huang *et al*., 2023). *scrib*/Dlg module is enriched with SJs and required for their assembly, whereas the correct apical localization of AJs is mediated by the Scrib component (Bonello *et al*., 2019; Zeitler *et al*., 2004; Harden *et al*., 2016). Thus, junctional network is a crucial component needed for maintaining epithelial ABP and tissue integrity.

1.5 The role of Scribble in cell proliferation

The Scribble module represents highly conserved neoplastic tumour suppressor genes from flies to humans (Carmena, 2020). The gene *scrib* encodes a protein that controls localization of other proteins through apical-basal axis (Bonello *et al*., 2019). Scribble is a multidomain scaffold protein, organised with 16 N-terminal leucine-rich repeats (LRRs), two LAP-specific, and four PDZ domains (Bilder *et al*., 2000). The research shows strong influence of the LRR domain on the establishment of the APB (Bonello & Peifer, 2019b; Huang *et al*., 2023). In order to study the effects of LRRs on the functioning of the *scrib*, the mutants with lacking or altered domains have been analysed. According to research findings, the LRRs tether Scrib to the plasma membrane. Expression of the LRRs is critical for polarising and

proliferation-controlling activity. Mutant proteins retaining LRR were able to shape an epithelial monolayer, while disrupted LRR led to alteration in tissue architecture (Zeitler *et al*., 2004b). In contrast, PDZ domain is not considered an essential determinant for regulation of epithelial organisation, however it functions as the binding sites for proteins, and it is involved in SJ formation (Bonello & Peifer, 2019). Lastly, *scrib* inhibits tumour progression as its loss results in hyperactivation of oncogenes like *yorkie* (Yki) in a Hippo pathway, and overgrowth of the tissue and neoplasia formation (Huang *et al*., 2023).

1.6 The importance of Hippo pathway in tissue homeostasis

Hippo signalling pathway is commonly acknowledged as a major regulator of tissue biology in development, homeostasis, and regeneration. The effects of the Hippo pathway are recognized in a wide range of processes, including early embryogenesis, cell differentiation, tissue repair, and stem cell and organ growth regulation (reviewed in Zheng & Pan, 2019). The Hippo pathway is a conserved signalling pathway observed in *Drosophila* and vertebrates. Mammals possess direct homologs/orthologs for all the core components in the *Drosophila* Hippo pathway (Halder & Johnson, 2011).

The Hippo signalling pathway is constituted by a core kinase cascade, guided by multiple upstream inputs, and has multiple transcriptional outputs (Dong *et al*., 2007). In fruit fly model organism, Hippo pathway central components are two serine/threonine kinases Hippo (Hpo) and Warts (Wts) together with their co-factors Salvador (Sav) and Mats, and the transcriptional co-activator Yorkie (Yki) and a transcriptional factor Scalloped (Sd) (Chen *et al*., 2020). In essence, Hpo together with Sav phosphorylates and activates Wts, which in turn phosphorylates Yki. Phosphorylation of Yki by Wts produces a 14-3-3 binding site, which promotes localization of Yki in cytoplasm, where it will subsequently go to degradation. In contrast, when Hippo pathway is inactive, Yki translocated into the nucleus, where it forms a complex with Sd to initiate the transcription of genes involved with proliferation, cell cycle progression (e.g., E-cyclin), and inhibition of apoptosis, which are necessary for tissue/organ growth (Dong *et al*., 2007). It was previously observed that cancer cells, overexpressing YAP (Yki homolog in vertebrates) are capable of escaping cell contact inhibition, which facilitates their ability to invade host tissues and metastasize (Zhao *et al*., 2007).

Hippo signalling is governed by a range of upstream signalling factors, including cell polarity maintenance, levels of F-actin, tension within the actin cytoskeleton, and cell attachments

(Gui *et al*., 2021). Several apical–basal cell polarity determinants were found to regulate the activity of the Hippo pathway. One example is the Crb protein that interacts with Hippo pathway component Expanded (Ex) and guides it to the apical membrane (Yu & Guan, 2013). Basolateral protein complex Scribble inhibits the Yki activity, by phosphorylating Yki and preventing its translocation into the nucleus. But the precise molecular mechanisms of this regulation are yet to be investigated (reviewed in Zheng & Pan, 2019b).

1.7 Cell-cell communication in tumorigenesis

Tumour development is a multistep process in which the interplay between oncogenic or tumour suppressor genes and the interactions between the affected and the adjacent wild-type (WT) cells is of great significance. Indeed, the regulation of tissue growth relies on cell-to-cell interactions and communication mediated by different transduction factors (reviewed in Enomoto & Igaki, 2022). Genetic studies in *Drosophila* imaginal discs revealed the role of oncogenic mutations driving tumour progression via cell-cell communications (reviewed in Rudrapatna et al., 2012). These genetic changes include endosomal sorting complex dysregulation, mitochondrial loss of function, apicobasal polarity disruption, and oncoproteins activation (Vaccari & Bilder, 2005; Ohsawa et al., 2012; Pagliarini & Xu, 2003; Enomoto et al., 2021).

In the wing imaginal disc epithelium, cell-to-cell interaction's dual role in tumour growth was previously discovered, where the loss of apicobasal polarity in the whole tissue due to the absence of Scrib or Dlg results in the overproliferation and cancer development (Bilder et al., 2000). In the scenario where polarity deficient *scrib* clones were surrounded by the WT (wild type) cells, they were found to be eliminated by neighbouring cells via apoptosis, leading to cell death, cell extrusion and engulfment of the mutant cells (reviewed in Bowling et al., 2019). Removal of the mutants is tightly connected to the levels of regulation of Yki, the transcriptional co-activator and downstream effector of the Hippo pathway (C. Chen et al., 2012a). On the other hand, other mutations in the cells can influence the fate of the polarity-deficient strains and promote apoptosis in WT cells (Moreno & Basler, 2004).

Notably, the recent research provides novel insights into the interactions between oncogenic and WT cells. The study revealed the effect of *scrib* RNAi-mediated conditional knockdown (KD) within the patched region (*ptc*) on the cells. The loss of the *scrib* was observed not

only in the target KD region but also in the flanking cells. At the same time, the prolonged knockdown time resulted in the disorganization of the whole tissue architecture (Gui et al., 2021). Additionally, suppression of the Yki signal did not rescue affected cells but did not spread further. The study suggests that ABP coordination either progresses or regresses through a novel mechanism termed "intercellular alignment of ABP" in a context-dependent manner (Gui et al., 2021).

Communication between cells is one of the critical mechanisms regulating epithelial growth and homeostasis. However, components mediating cell-to-cell interactions together with Scrib still need to be explored.

1.7.1 Cell competition contribution in ABP maintenance

Cell-to-cell competition was found to protect the tissue from tumorigenesis. In essence, cell competition is a context-dependent cells interaction whereby cells with higher fitness eliminate neighbouring cells with lower fitness by inducing apoptosis (Kanda & Igaki, 2020). Within the wing imaginal disc of D. melanogaster, the spread of *scrib* null allele cells in the tissue is restricted by the WT cells, eliminating the mutants (C. Chen et al., 2012). Loss of APB determinant in the mutants leads to elevated expression of Yki (Doggett et al., 2011). WT cells inhibit overproliferation in tumorous cells by suppressing Yki activity (C. Chen et al., 2012b). Suppression is achieved through cell competition, which activates apoptotic JNK pathway in *scrib* mutant cells (Brumby & Richardson, 2003b). The JNK pathway is triggered by Eiger, the Tumour Necrosis factor (TNF) in fruit flies, together with its receptor Grindelwald. Due to the increase in levels of endocytosis in tumour cells, the TNF is translocated to the endosomes from the plasma membrane, activating apoptosis pathway (Kanda & Igaki, 2020b). JNK signaling antagonizes Yki activity, and the mutant cell is removed. Conversely, the Yki activity is upregulated in neighbouring cells, thus resulting in non-compensatory proliferation (Kanda & Igaki, 2020).

Notably, the overexpression of one pro-proliferative factor, Myc, influences the mutant cell's ability to evade the elimination, stimulating the apoptosis of surrounding cells (reviewed in Bowling et al., 2019). However, the survival of the *scrib* null-allele mutants expressing Myc was not connected to a cell-autonomous increase in proliferation rate. Instead, the determining element appeared to be the relative level of Myc produced in the clone cells compared to the expression in the WT cells (C. Chen et al., 2012).

1.7.2 Intercellular alignment components and mechanism in ABP coordination

Proper tissue development relies on the APB establishment and maintenance. The process of ABP signal transmission across the tissue was termed "intercellular alignment". The interactions between sub-optimal (oncogenic)/optimal (WT) cells can be directed not only to the elimination of carcinogenic cells but also to the integration of the cells in tissue due to progressive loss or establishment of the ABP (Gui et al., 2021). For instance, hypomorphic mutants for *scrib* can be rescued from loss of polarity by other cells, retaining the essential LRR domain in the protein (Gui et al., 2021; Khoury & Bilder, 2020). In contrast, when expression of the *scrib* was entirely dismissed through the RNAi KD in the *ptc* region, the loss of ABP determinant expanded to the flanking cells, promoting overproliferation. In addition, the dosage of *scrib* has a differential impact on tissue architecture and overall growth (Gui et al., 2021; Huang et al., 2022). The reason behind this could be the balance between tissue growth and homeostasis for proper tissue development (Huang et al., 2022).

The ABP alignment signal is transmitted within the tissue through cell connections with the *scrib* assistance. In *Drosophila* wing imaginal disc, *scrib* sustains the tissue homeostasis through cell-to-cell communication by genetic and physical interactions with SJs complex and α-Cat. Previously it was stated that the α-Cat functions at the AJs, while the recent experiments show that some α-Cat also resides at SJs and regulates Yki activity through *scrib*, and, together with SJs, controls the *scrib* localization (Figure 5) (Huang et al., 2023).

In conclusion, cell interactions aid the restoration or loss of ABP polarity, inherently impacting tissue homeostasis and architecture. Scrib assists in relaying the ABP signal through the tissue, interacting with α-Cat and SJs.

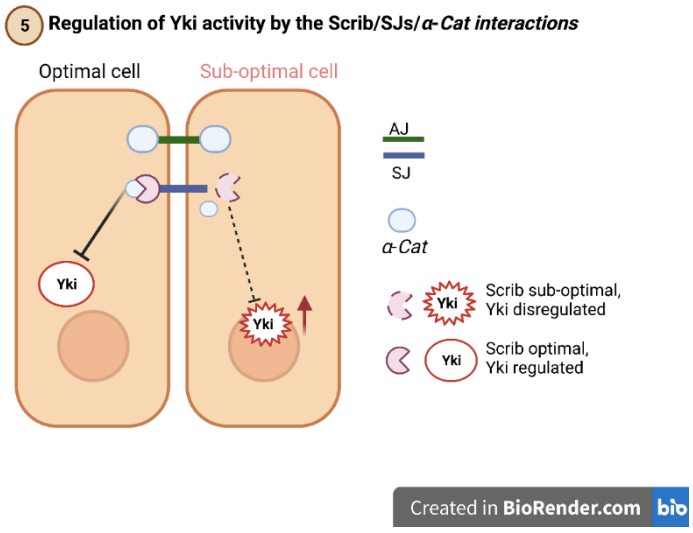

Figure 5. Regulation of Yki activity by the Scrib/SJs/ *α-cat*: based on Huang *et al.*, 2023.

SUMMARY

D. melanogaster is a favoured model organism to study disease processes, given the homology between insects and mammals, the variety of genetic tools, and the rapid life cycle. Notably, the unique properties of the wing disc, including its structure (a monolayer of the columnar epithelium) and its rapid growth rate during development, compose a promising model system to research excessive proliferation and cancer development. By utilizing the UAS/GAL4/GAL80^{TS} in the simplified model of the tissue structure, and imaginal disc, the development of the epithelial tissue against a visualized protein of interest can be examined. Importantly, combining the UAS/GAL4/GAL80^{TS} system together with RNAi enables to silence of the protein, therefore providing a tool to study conditional knockdown. In the experimental part of this research, *scrib* RNAi is used to disrupt the epithelial tissue polarity partly. Since Scrib is the major ABP determinant and a known tumour suppressor gene, loss of polarity in the tissue is expected. The system of UAS/GAL4/GAL80^{TS} + RNAi is regulated by the patched (*ptc*) enhancer domain, allowing to express the construct in a tissue-specific manner and according to the temperature shift. Hence, UAS/GAL4/GAL80^{TS} + *scrib* RNAi system provides a convenient platform to study the *scrib* knockdown at different time inductions in the wing disc of larvae.

In the intercellular alignment concept, the importance of cell-to-cell communication is highlighted. By introducing *scrib* RNAi KD in the group of cells, the progressing loss of polarity in the target and adjacent cell populations was observed. The interactions between *scrib*-RNAi KD and WT cells reveal the role of Scrib in establishing intercellular alignment. Scrib interacts with α-Cat and SJs to relay the ABP signal in the neighbouring cells. Yet the precise mechanisms underlying such communications are not identified. In order to clarify the possible Scrib-involved molecular network mechanisms in tissue growth and homeostasis, genes synergetic with *scrib* should be investigated. To explore possible interactions, image-based screening in the fruit fly's specific genomic regions (deficiency lines) in the wing imaginal disc could be conducted.

2 THE AIMS OF THE THESIS

Based on previous studies, the tumour suppressor gene and the key ABP determinant, Scrib, mediates the intercellular alignment of the polarity within the tissue through cell-to-cell interactions. Recent findings revealed that α-Cat and SJs are involved in intercellular interactions in Scrib-mediated tissue homeostasis, indicating the involvement of numerous genes in the process (Huang *et al*., 2023). Therefore, in this thesis, the synergy of *scrib* with other genes is hypothesized. To identify genes interacting with *scrib*, the following research question was set.

- Which potential genes on the right arm of the third chromosome could contribute to regulating tissue homeostasis by maintaining ABP and having synergy with *Scrib-ble*?
    - This study aims to carry out a screening of deficiency lines of the third chromosome in *Drosophila melanogaster* to identify candidate genes having genetic interactions/synergy with *scribble*.
    - To achieve the goal, UAS-GAL4/GAL80 system with *scrib* RNAi knock-down was utilized to carry out a two-step screening experiment for identifying novel candidate genes, interacting with *scrib*.

3 EXPERIMENTAL PART

3.1 MATERIALS AND METHODS

3.1.1 *Drosophila* lines used and preparation for screening experiments

In Table 1 all fruit lines that have been used in the screening experiments are listed. The laboratory stock was used as the driver line to introduce the RNAi knockdown of the *scrib* gene. The *ptc-Gal4* driver sequence was utilized to express *scrib* RNAi cells in a thin stripe at the border of A/P compartments. The RNAi mechanism is explained in Figure 6**.**

Table 1. *Drosophila* lines used for crossing.

Stock number (Bloomington)	***Line genotype***	***Source***
N/A	*ptc*-Gal4,UAS-GFP, ex-LacZ/CyO; UAS-*scrib*RNAi,Gal80^{TS}/Tm6BTbSb	Laboratory stock
23232	w[*]; ry[506] Dr[1]/TM6B, P{Dfd-GMR-nvYFP}4, Sb[1] Tb[1] ca[1]	Bloomington *Drosophila* Stock Centre (BDSC)
8105	w[1118]; Df(3R)ED6232, P{w[+mW.Scer\FRT.hs3]=3'.RS5+3.3'}ED6232/TM6C, cu[1] Sb[1]	BDSC
2352	Df(3R)X3F, P{ry[+t7.2]=RP49}mtg[P2] e[1]/MKRS	BDSC
8685	w[1118]; Df(3R)ED7665, P{w[+mW.Scer\FRT.hs3]=3'.RS5+3.3'}ED7665/TM6C, cu[1] Sb[1]	BDSC

8967	y[*] w[1118]/Dp(1;Y)y[+]; Df(3R)ED5147, P{w[+mW.Scer\FRT.hs3]=3'.RS5+3.3'}ED5147/TM6C, cu[1] Sb[1]	BDSC
9082	w[1118]; Df(3R)ED5474, P{w[+mW.Scer\FRT.hs3]=3'.RS5+3.3'}ED5474/TM6C, cu[1] Sb[1]	BDSC
9500	w[1118]; Df(3R)BSC140/TM6B, Tb[+]	BDSC
7681	w[1118]; Df(3R)Exel6202, P{w[+mC]=XP-U}Exel6202/TM6B, Tb[1]	BDSC
9090	w[1118]; Df(3R)ED5644, P{w[+mW.Scer\FRT.hs3]=3'.RS5+3.3'}ED5644/TM6C, cu[1] Sb[1]	BDSC
7731	w[1118]; Df(3R)Exel6264, P{w[+mC]=XP-U}Exel6264/TM6B, Tb[+]	BDSC
27921	w[1118]; Df(3R)BSC849/TM6C, Sb[1] cu[1]	BDSC
27360	w[1118]; Df(3R)BSC788/TM6C, Sb[1] cu[1]	BDSC

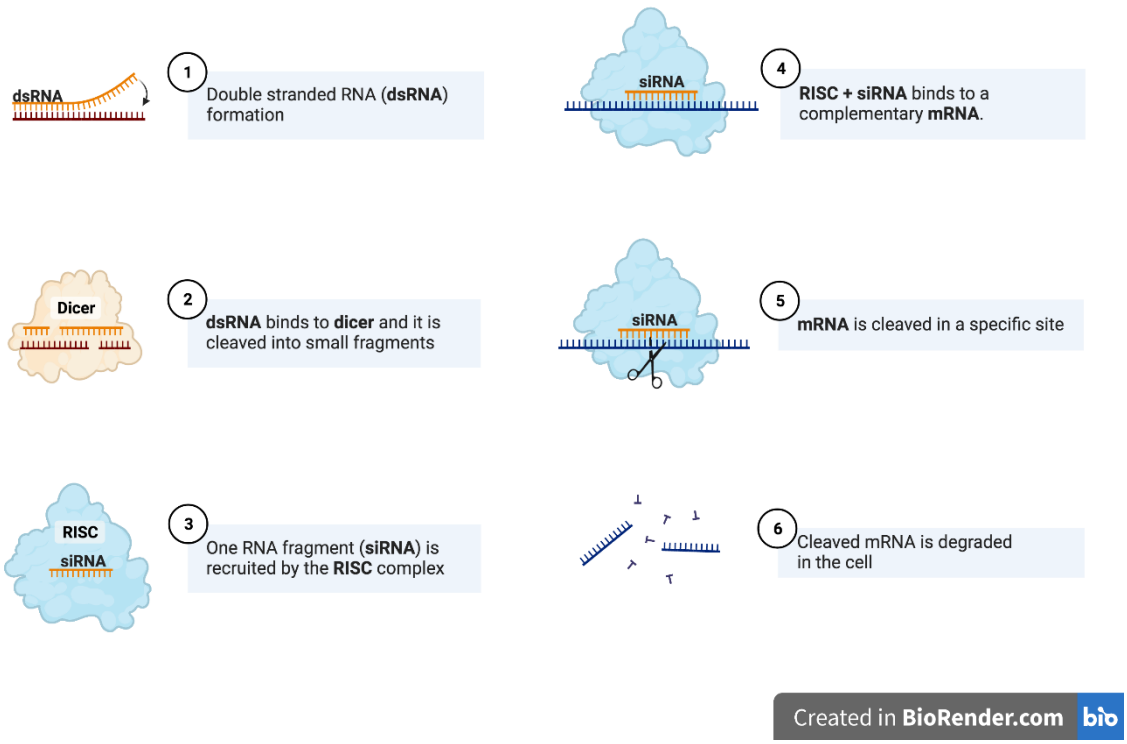

Figure 6. RNA interference mechanism. The double-stranded RNA (dsRNA) is cleaved, forming single-stranded small molecules known as siRNA. Then the siRNAs associate with the RISC complex. The siRNA targets its complementary mRNA in a specific manner, promoting binding and subsequent degradation of the mRNA molecule.

UAS/GAL4/GAL80 system was used to gain the tissue-specific expression of the target gene. Expression of GAL4 is controlled through the temperature shift since GAL4 repressor GAL80 is a temperature sensitive mutant. To preserve of the initial genotype and to avoid the homologous recombination events, the second chromosome balancer Cyo (curly wings) and the third chromosome balancer Tm6TBSb were combined. Additionally, laboratory stock contains Ex-LacZ (Expanded-lacZ), which allows to visualize Yki activity and UAS-GFP to visualize GAL4 expression.

To receive the final stock with the deficiency line and *scrib* conditional knockdown the following crossing procedure was used. The crossing procedure included several steps. Firstly, the deficiency lines of interest were checked for the specific balancer in their genotype. The desired balancer in the deficiency lines was TM6TBSB, since it has a dominant marker Tubby, which shows a shorter body phenotype during larval stage. The significance of this step lies in the ability to easily pick-up the correct genotype after crossing with *scrib*-RNAi-

host stock. If the deficiency line possesses TM6TBSB in its genotype, then the next step, setting up cross with the Scrib-host stock was done **(Figure 7).**

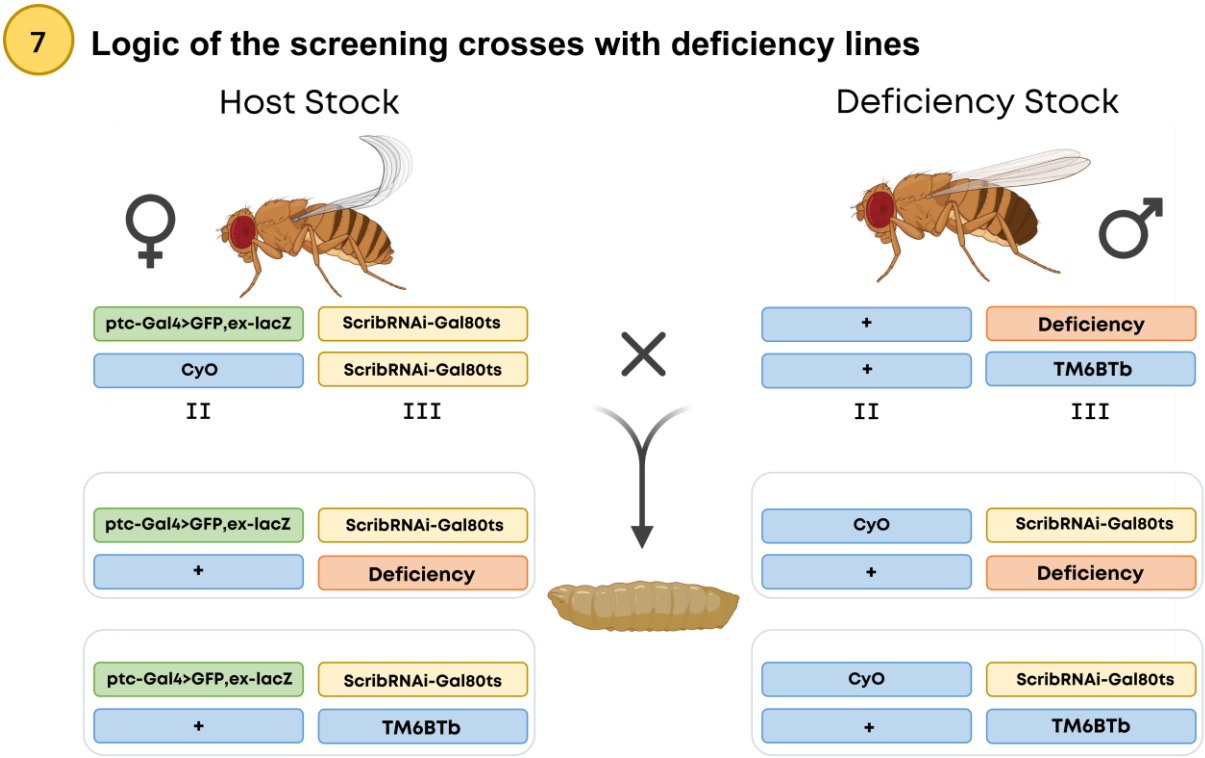

Figure 7. Logic of the screening crosses with deficiency lines.

If the deficiency line of interest did not have the desired balancer in the genotype, then prior to crossing with the *scrib*-RNAi host stock, the changing of the balancer took place. To change the initial balancer to the TM6TbSb, the cross of the deficiency line with the line number 23232 was done. The genotype of 23232 has two phenotypic markers: the small eyes from the gene Dr and the Tb (tubby) larvae from the gene TB. In the adult fly stage, the TM6TbSb balancer marker is expressed in the presence of short hair on thorax due to dominant marker Sb. Therefore, after setting up a crosses between the deficiency line and 23232, the flies, which show the correct phenotype – normal-sized eyes and short hair on the thorax, – were collected. To preserve the desired genotype, the flies were self-crossed. Afterwards, the stable stock of Deficiency line (Df)/TM6TBSB is obtained and then crossed with the *scrib*-RNAi host-stock to initiate the *scrib* knockdown.

For observing variations, that are because of mutations in the *scrib*-host RNAi stock the positive control (+) was added. The positive control was prepared for the screening with self-

crossing of the *scrib*-RNAi. The control was labelled as positive, since previously the introduction of 2D KD (2 days after temperature shift) resulted in the slight expansion of the polarity loss signal in the anterior part (Huang *et al.*, 2023). Nevertheless, only a slight phenotype is expected at 2D under 2 copies of *scrib* genes in the laboratory stock. Apart from positive control, the positive-positive control is added to be screened together with Df line and positive control. The positive-positive (++) control represents one Df line 8105, containing deficiency of *scrib* locus. Together with Scrib RNAi KD that was introduced, this line was expected to show severe phenotypes.

3.1.2 Conditional knockdown procedure

Flies were raised on a standard medium, with additional yeast in order to facilitate egg laying. Afterwards, the crosses of the *scrib*-RNAi stock with Df line were set, and flies were left at 18℃ for 12 hours for egg laying. After that, several induction periods were used to observe the *scrib*-RNAi knockdown effect together with Df line at different stages.

Based on previous studies, the prolonged knockdown leads to more cells losing the APB polarity (Gui *et al*., 2021).

Therefore, to observe the tissue at different stages of development, several time induction protocols were implemented. The following table shows all time points, that were tested:

Table 2. Conditional knockdown.

Growth stage (18℃)	***Knockdown induction (29℃)***
4.5 days	2 days
4 days	2 days
3 days	3 days
1.5 days	4 days

For the primary screening of crosses, the following conditions were used (Table 2). Firstly, the crosses were put at 18°C for 4 days, then they were shifted for 2 days at 29°C.

According to the recent findings, the loss of polarity in the discs at 2D RT can be observed only in the anterior domain (Gui *et al*., 2021). Therefore, if the Df line displays a more severe phenotype, with extension of the GFP signal to the posterior part, then the *scrib* synergy event occurs and some deleted genes from the Df line were important to maintain the polarity together with *scrib*. The protocol was further adjusted to 3D time induction, in order to enhance the phenotypic difference between the Df lines and control lines, that were screened together with the line of interest.

During secondary screening, the protocol of 3D to 3D was performed to differentiate the resulted phenotype between the controls and the deficiency line. Additionally, with the candidate line, the protocols of 4.5/2D, 1.5/4D were used to observe the development of the tissue at different time points.

3.1.3 Screening workflow

Subsequently, wing imaginal discs were dissected, fixed, stained, and prepared for imaging. Firstly, only the deficiency lines with *scrib* RNAi host stock were dissected; afterwards, the protocol was improved, *scrib*-host stock (+) and Df 8105 (++) control lines were added to the experiment each time. This was done to enhance understanding of factors behind variation in phenotype and to create finer visualisation of the results**.** Firstly, the primary screening was conducted. The main purpose of the primary screening was to determine the candidate lines. Thus, the staining with DAPI was carried out. In the case of a candidate line showing a positive phenotype, the screening experiment (secondary screening) was carried out again with additional staining to observe and analyse the altered expression of proteins essential in the disrupted tissue homeostasis. The first one, anti-β-Galactosidase was used as a secondary antibody to stain Ex-LacZ which serves as a reporter for Yki activity. (Yu & Pan, 2018) Additionally, anti-Dlg antibody was employed to stain Dlg protein, which acts as a tumor-supressor along with *scrib* and forms basolateral complex in epithelial cells. (Woods et al., 1996) Lastly, De-Cadherin was stained with antibody DCAD2. De-Cadherin, a *Drosophila* homolog for E-Cadherin, is a core component of the AJs, that regulates cell-cell adhesion and, therefore, the maintenance of ABP. (Jaiswal et al., 2006)

3.1.3.1 Dissection and fixation

The third instar larvae were collected from the vials and checked for expression of GFP signal in salivary glands under confocal microscope. The GFP-positive larvae were transferred into 1x Phosphate-buffered saline (1xPBS) and placed on ice to reduce larvae movement. Next, the larvae were dissected so the wing imaginal discs were exposed and collected in a 1xPBS Eppendorf tube. The tissue fixation was done with 3.7% formaldehyde solution in 1xPBT (0.1% Tween20 in 1XPBS). The samples were incubated in the fixation solution (FS) for 20 minutes at RT. Then the FS was removed with the pipette, and the samples were washed two times with 1xPBT.

3.1.3.2 Staining

When the primary screening was performed, the samples were stained with the specific DNA dye, DAPI, at a concentration of 1:300. The samples were kept in the dark and were stained for 30 minutes in the RT or overnight at 4°C. Next, the discs were washed with 1xPBT three times.

During the secondary screening, prior to staining, the samples were blocked in 5% Goat Serum in 1XPBT for 2 hours at RT. Then the primary antibody of choice was added to the blocking solution in concentrations as follows: anti-β-galactosidase (1:500), anti-discs large and DCAD2 (1:50) and incubated overnight at 4°C. The following day samples were washed three times with 1xPBT with time intervals of 10 minutes. The secondary antibody of choice was added in 1:200 concentration to the tubes with discs and 1xPBT. The samples were incubated for 2 hours at RT in a dark place and were then washed with 1xPBT two times with an interval time of 10 minutes.

The following secondary antibodies were implemented during experiments: Alexa Fluor® 647 Goat anti-mouse IgG (Thermo Fisher Scientific), Alexa Fluor® 568 Goat anti-mouse IgG (Thermo Fisher Scientific), and Alexa Fluor® 568 Goat anti-rat IgG (Thermo Fisher Scientific).

In the next step, DAPI was added (stock solution concentration: 1mg/ml) at a concentration of 1:300 and incubated at RT in a dark place for 30 minutes. Following incubation, samples

were washed with 1xPBT twice. The discs were further dissected in 1xPBT, to remove excessive body parts, mounted and imaged.

3.1.3.3 Mounting

Microscope slides were prepared by cleaning the surface with 70% ethanol. The discs were transferred with a pipette on the slide, excessive PBT was removed, and a drop of 70% glycerol was added to the sample. The coverslips were put on the slides, and transparent nail polish was applied to the borders of the coverslip to fix the slide.

3.1.4 Imaging and image analysis

The fluorescence microscope **(*Olympus BX51 Fluorescence Microscope* | *Olympus LS*, n.d.)** was used to achieve high-quality images. The fluorophore-labelled cell components are visible due to the high-energy and short-wavelength light generated by the mercury arc vapour lamps and directed through an excitation filter, allowing only specific short-wavelength light to move across it. The filtered light is reflected on the dichroic mirror and directed to a specific fluorophore of interest. The samples were viewed under a 20x microscope objective.

The preparation of pictures and editing was done in ImageJ/Fiji with a macro plugin. This software was implemented for merging two channels and adding a scale bar on the pictures.

3.2 RESULTS

3.2.1 Systematic primary screening

In this experiment, the wing imaginal discs of third stage larvae of the Df lines were used. Df lines were ordered from BDSC and were missing some genomic region in the chromosome. The information about eliminated genes from the region was found at the BDSC. For the purpose of determining the specific genomic regions/alleles, which presumedly have genetic interaction with *scrib*, the primary screening experiment of the Df lines was conducted.

During primary screening, all wing discs were stained with the DNA-dye, DAPI, which allowed to observe the localization of the cells across the tissue and with GFP, which would stain cells in the *ptc* region. Within the wing imaginal discs pictures that were received, the expression of *scrib*-RNAi-affected cells was regulated by the *ptc* sequence; As a result, the cells were expressed in the stripe on the boundary of A/P domains (Figure 8). The structure of the discs composed of three main regions: Notum, Hinge-pouch, and pouch domains, shaping the morphology of the discs (Figure 8). In contrast, when the three regions are disorganised and the GFP stripe of cells is intensely expanded, the formation of the neoplastic structure is expected.

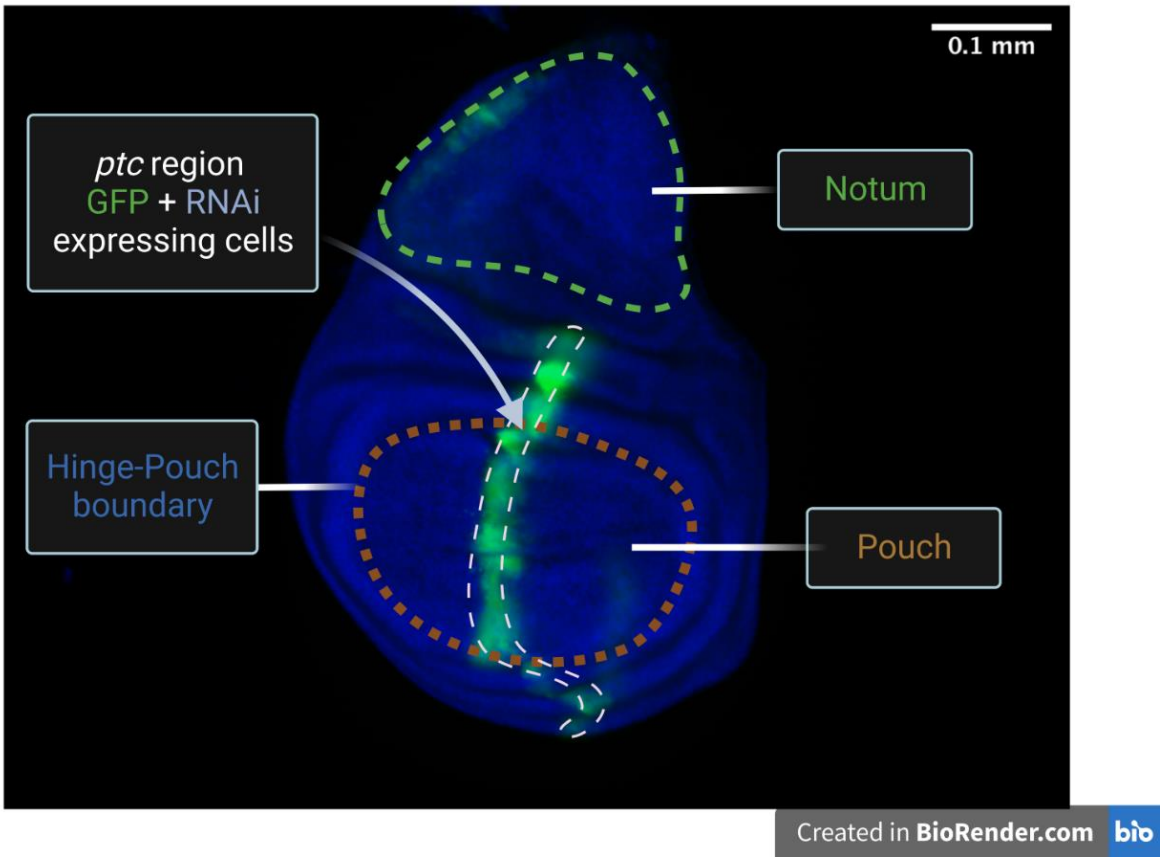

Figure 8. The wing imaginal regions. The figure shows three essential domains within the wing imaginal disc: pouch region (brown dashed line), hinge-pouch boundary (border of the brown dashed line) and notum (green dashed line). DAPI (blue) stains the DNA of the cells, and GFP (green) shows the expression of the affected cells in the *ptc* domain by the RNAi-induced KD of the *scrib*.

The systematic primary screening of the Df lines included 10 different Df lines screening. At 2D ATS, 4 Df lines did not show the strong phenotype. The stripe of RNAi KD cells did not move to other compartments from the *ptc* domain. The structures of the discs (hinge, notum, hinge-pouch) were clearly visible (Figure 9).

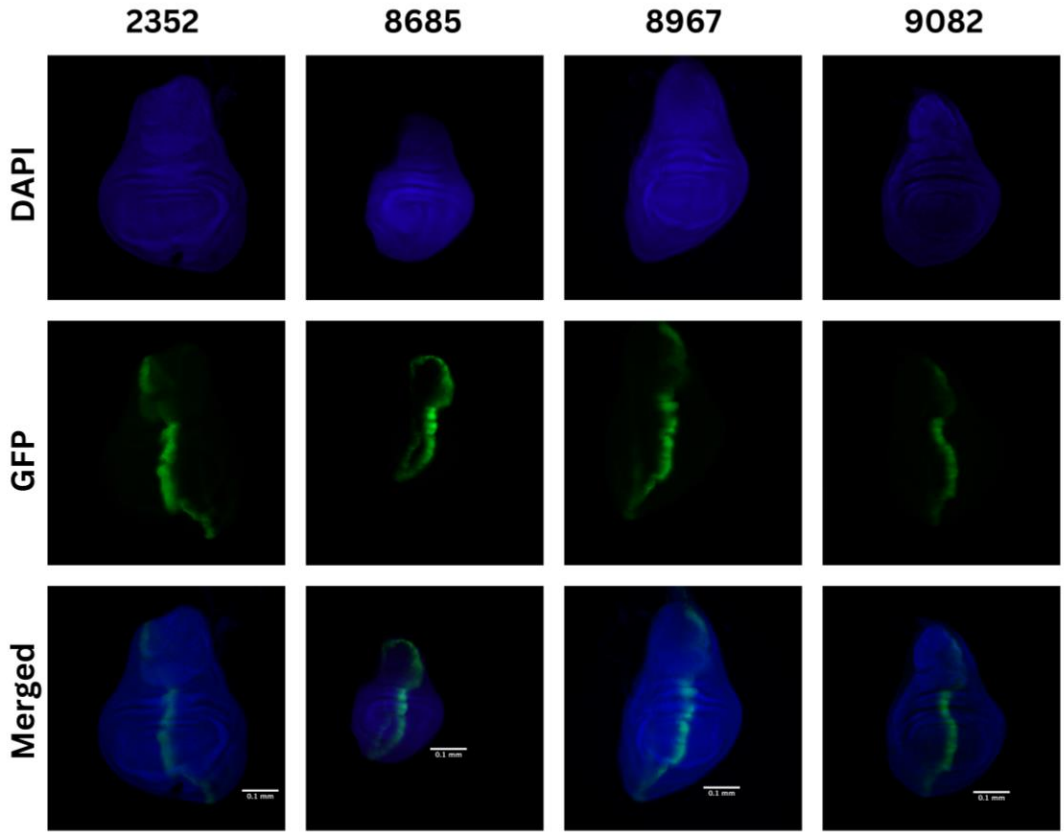

Figure 9. **Primary screening negative candidates.** Four different Df lines (2352, 8685, 8967, 9082) were stained with DAPI (blue). The GFP stripe (the expression of the affected cells by the RNAi-induced KD of the *scrib*) is shown in the A/P stripe (green); the merged image of GFP and DAPI was created in ImageJ. The KD induction time is 2D ATS (after temperature shift). The DNA is visualised with DAPI. Scale bar: 0.1 mm.

The following results in Figure 9, suggest that these Df lines were not experiencing strong polarity loss and likely do not have synergetic interactions with *scrib*.

During the primary screening, one potential Df line candidate (7681) out of 10 was examined. In Figure 10, the GFP stripe of *scrib*-RNAi KD cells has expanded not only in the anterior domain but also in the posterior region. Following these results, the loss of the essential gene interacting with *scrib* can be hypothesised.

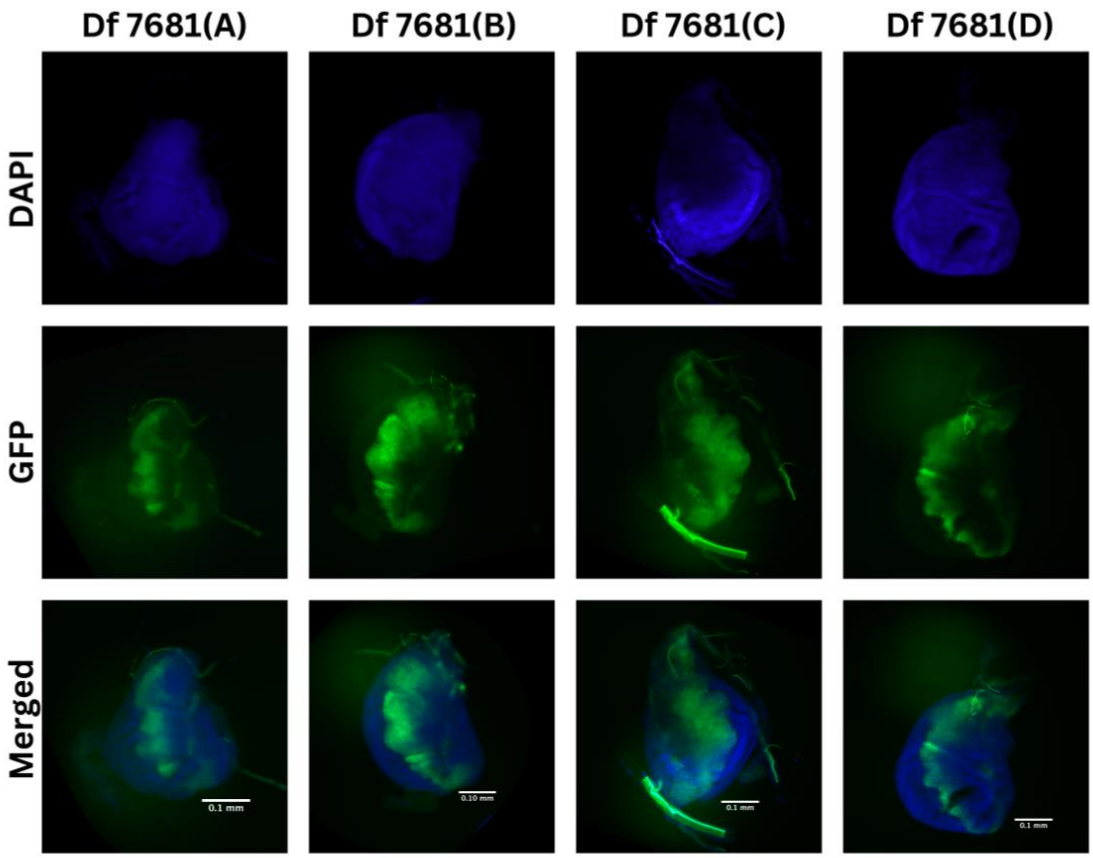

Figure 10. **Primary screening positive candidate.** Df line 7681 stained with DAPI (blue) and GFP (green). The deficiency line different wing discs are marked with A, B, C, D. A merged image of GFP and DAPI is created with ImageJ. The KD induction time is 2D ATS (after temperature shift). The DNA is visualised with DAPI. Scale bar: 0.1 mm.

3.2.2 The 7681 positive candidate secondary screening

In order to test the levels of Yki activity in the positive candidate deficiency line, ex-LacZ staining was carried out (Figure 11). In addition, two controls: positive and positive-positive, were added to the screening experiment (Figure 11). This was done to better understand the variability behind the phenotype. In Figure 11, the results of the secondary screening are shown.

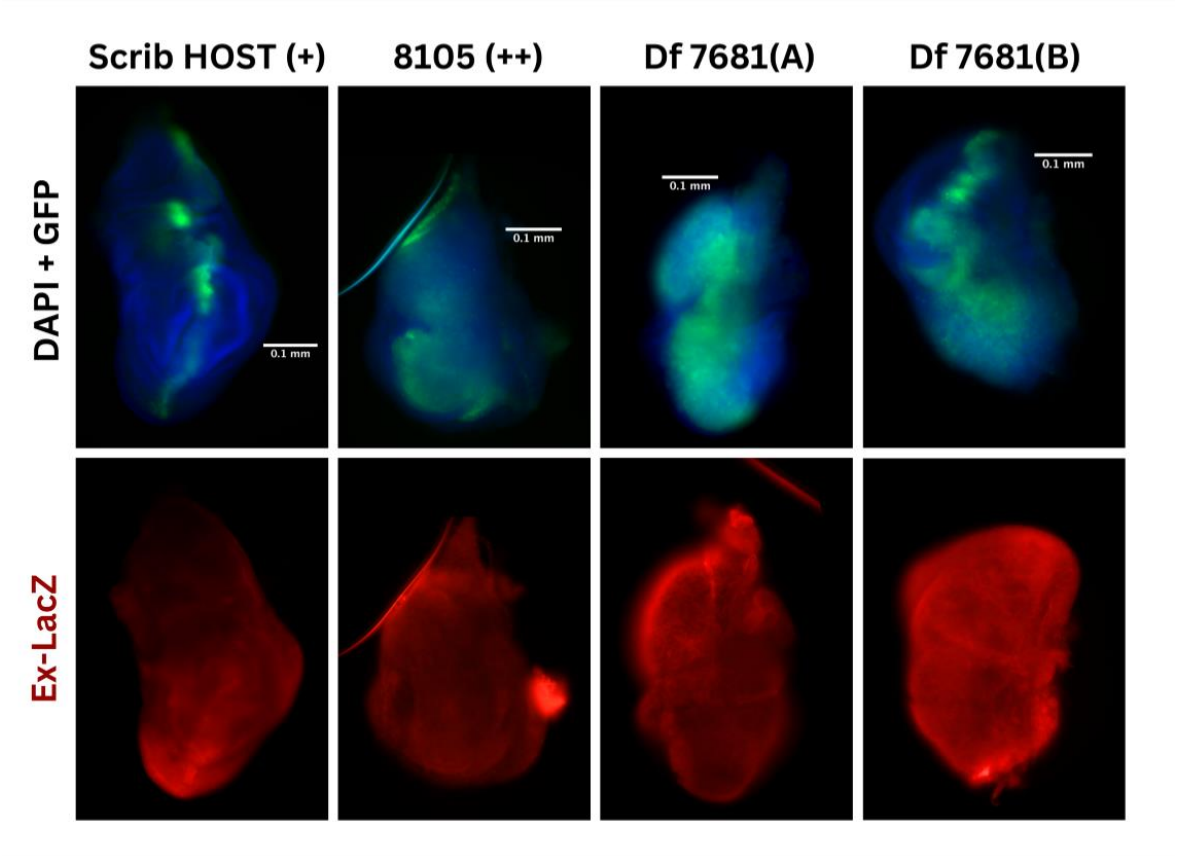

Figure 11. The secondary screening of the 7681. The secondary screening of the 7681. The first two columns depict two controls: positive (+) and positive-positive (++). The A and B refer to two different discs of the deficiency line 7681. The discs were stained with DAPI (blue) with GFP expression (green). Secondary antibody: anti-β galactosidase was used to express ex-Lacz, which serves as a Yki readout. The time induction used: 3D ATS. Scale bar: 0.1 mm.

The positive (+) control does not show tissue disorganisation and high activities of Yki (Figure 11). However, a slight expansion of the GFP signal is observed. This might be due to the KD time of 3D, since in the previous studies already at 2D, the expansion of the stripe was

observed (Gui et al., 2021). The deficiency line of interest (Figure 10A and B) shows severe overproliferation and high activity of the Yki.

Hence, the 7681 Df line remained a strong candidate, which was greatly affected by the *scrib* RNAi KD, indicating that some genes eliminated from the fly genomic region, were essential to maintain tissue organization together with *scrib*.

3.2.3 The narrowing of the gene region

In order to limit the number of potential genes, interacting with *scrib*, two lines with overlapping deleted genomic regions were selected for the screening experiments. In FlyBase database, it was found that Df line 7681 overlaps only with 4 lines, whereas two of them share most of the genes deleted, the third one overlaps only with 7681 and at a small region. The fourth one, Df line 27360 overlaps with the primary candidate and the Df 27921. (FlyBase, n.d.).

The region of deleted genes of the positive candidate 7681 was analysed, therefore two overlapping Df lines regions were utilised for the next screening experiments. Df 27921 and Df 27360 were implemented to reduce the number of genes. The two lines with wide and short genomic regions were chosen, therefore, to narrow down the number of possible genes to 10 coding sequences if both lines were found to be positive candidates (Figure 12).

Figure 12. Df line 7681 genomic regions with four overlapping deficiency lines. Yellow line: deleted gene region for the primary candidate Df line 7681. Brown lines: deleted regions of two Df stocks that were employed to reduce number of genes.

3.2.4 Primary screening results

The primary screening for both lines was performed, and the results are shown in Figures 13 and 14.

In Df line 27921 the GFP signal expanded across the tissue, depicting tumorous phenotype. The wing structures were lost.

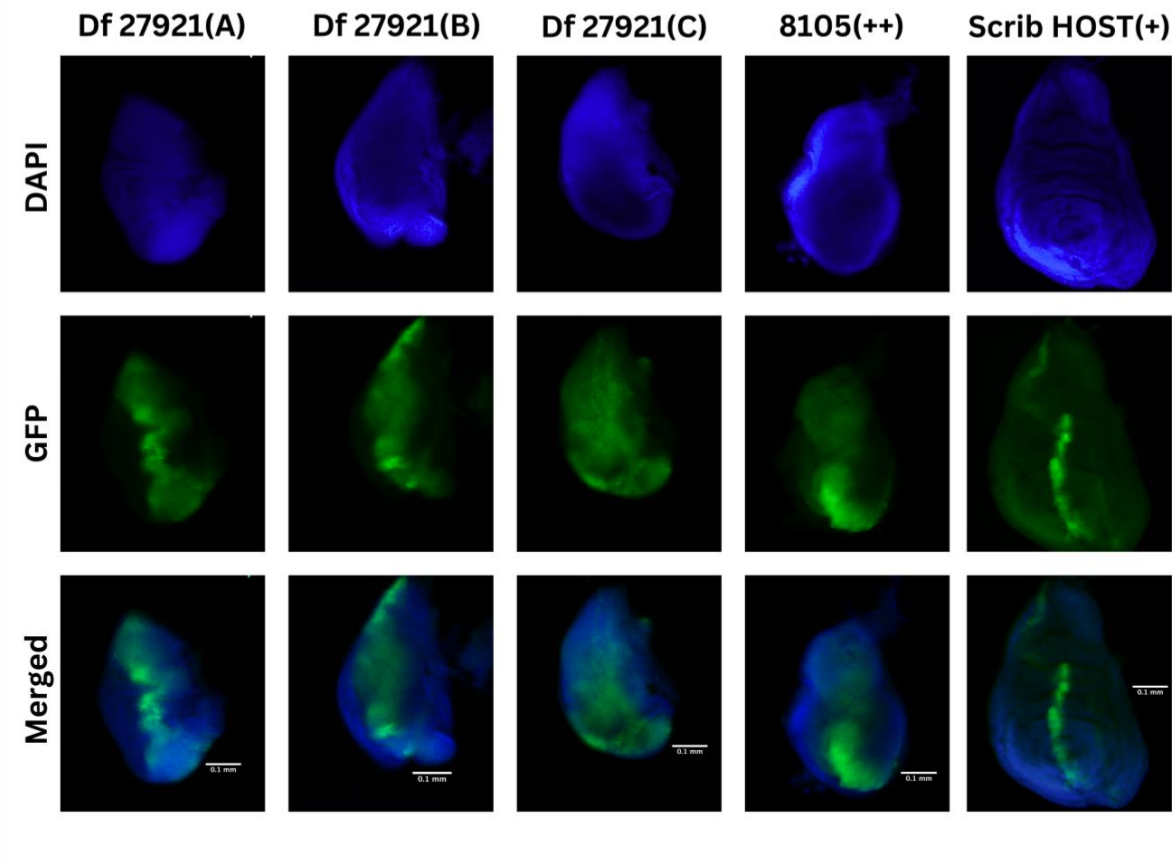

Figure 13. The primary screening results for positive candidate, Df line 27921. Df line 27921 stained with DAPI (blue) and GFP (green). The deficiency line different wing discs are marked with A, B and C. The last two columns are the positive-positive (++) and positive (+) controls. A merged image of GFP and DAPI is created with ImageJ. The KD induction time is 3D ATS. The DNA is visualised with DAPI. Scale bar: 0.1 mm.

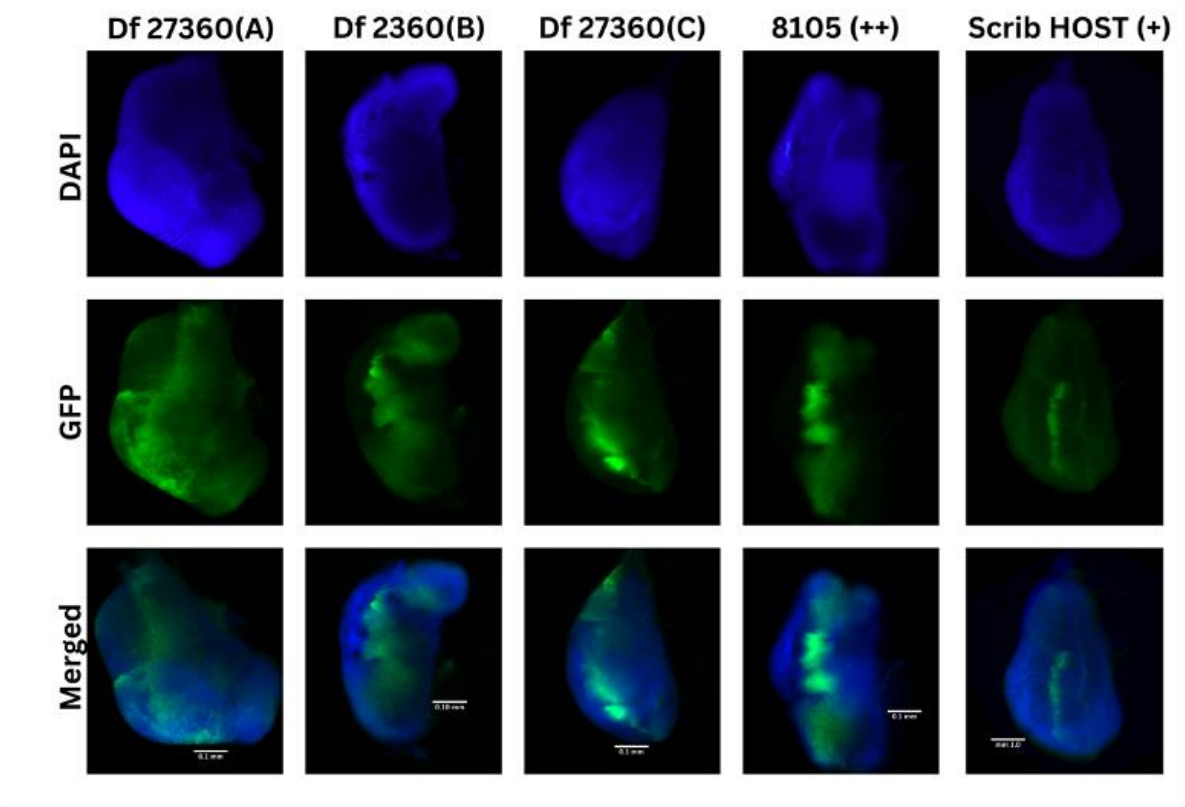

Figure 14. The primary screening results for positive candidate, Df line 27360. The primary screening results for positive candidates, Df line 27360. Df line 27360 stained with DAPI (blue) and GFP (green). The last two columns are the positive-positive (++) and positive (+) controls. The deficiency line different wing discs are marked with A, B and C. Merged image of GFP, and DAPI is created with ImageJ. The KD induction time is 3D ATS. The DNA is visualised with DAPI. Scale bar: 0.1 mm.

3.2.5 Positive candidate Df line 27360 secondary screening

With the purpose of screening the activity of Yki, ex-LacZ staining was performed. The results are shown in the Figure 15. In Figure 15, presented wing imaginal discs are experiencing proliferation to a different extent, including *scrib*. The ex-LacZ is expressed at elevated levels within the tissues, which indicates the hyperactivation of the Yki. Notably, the positive (+) and positive-positive (++) controls experienced overgrowth, while Df line discs were small, and the GFP signal was dispersed across the tissue. This could be an indicator of the late neoplastic stage, since the GFP signal potentially diffused through the tissue, denoting the possible migration of epithelial cells. In relation to this, the tissue architecture could be altered into the folded mass of cells. The positive control experienced overgrowth as well, which could be the result of a balancer loss in the stock, which has increased the RNAi dosage in the genotype.

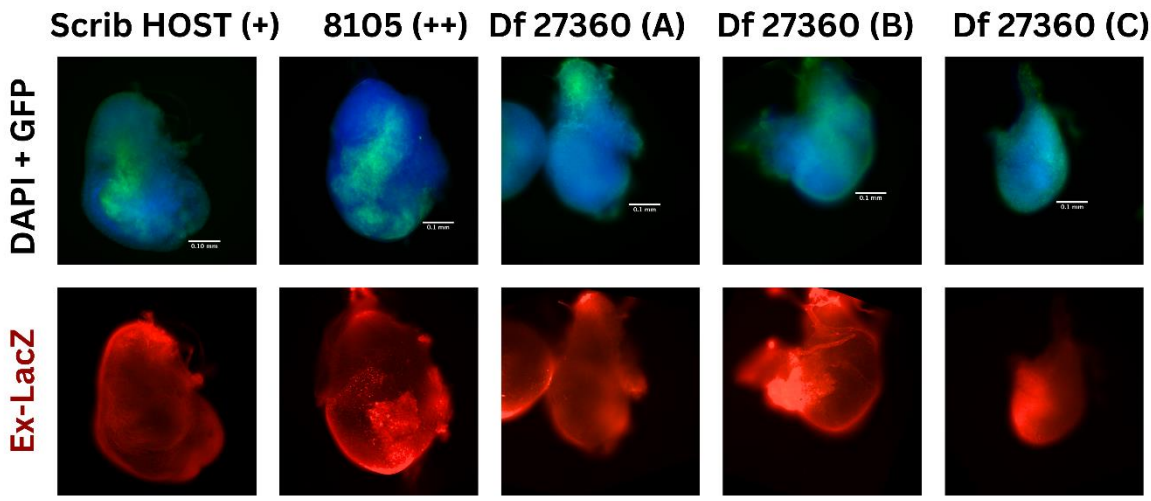

Figure 15. The secondary screening of the Df line 27360. The secondary screening of the Df line 27360. The first two columns depict two controls: positive (+) and positive-positive (++). The A, B, and C refer to three different discs of the deficiency line 27360. The discs were stained with DAPI (blue) with GFP expression (green). A merged image of GFP and DAPI is created with ImageJ. Secondary antibody: anti-β galactosidase was used to express ex-Lacz, which serves as a Yki readout. The time induction used: 3D ATS. Scale bar: 0.1 mm.

3.2.6 Positive candidate Df line 27360 induction times

Different KD time inductions were tested in the positive candidate 27360 to observe tissue development and loss of polarity at different stages. The results are presented in Figure 16. The results shown in Figure 16 show the progressive neoplasia formation in the wing imaginal discs with the prolonged time of *scrib* knockdown. Notably, at 3D ATS, both the Df line and positive-positive control (++) experienced strong expansion of the stripe, consequently loss of polarity, while the positive (+) control did not exhibit the strong phenotype and did not relay the ABP regression from the initial KD region. Nevertheless, at 4D ATS, the *scrib* HOST stock experienced the strongest overgrowth, and this resulted in disruption of the tissue architecture. At 2D ATS, the tissue structure is maintained in all fly lines. However, the GFP stripe of Df line 27360 and positive-positive control has already expanded, indicating the wing disc *ptc* domain RNAi KD of Df line 27360 and positive-positive (++) control has interacted with the flanking WT cells.

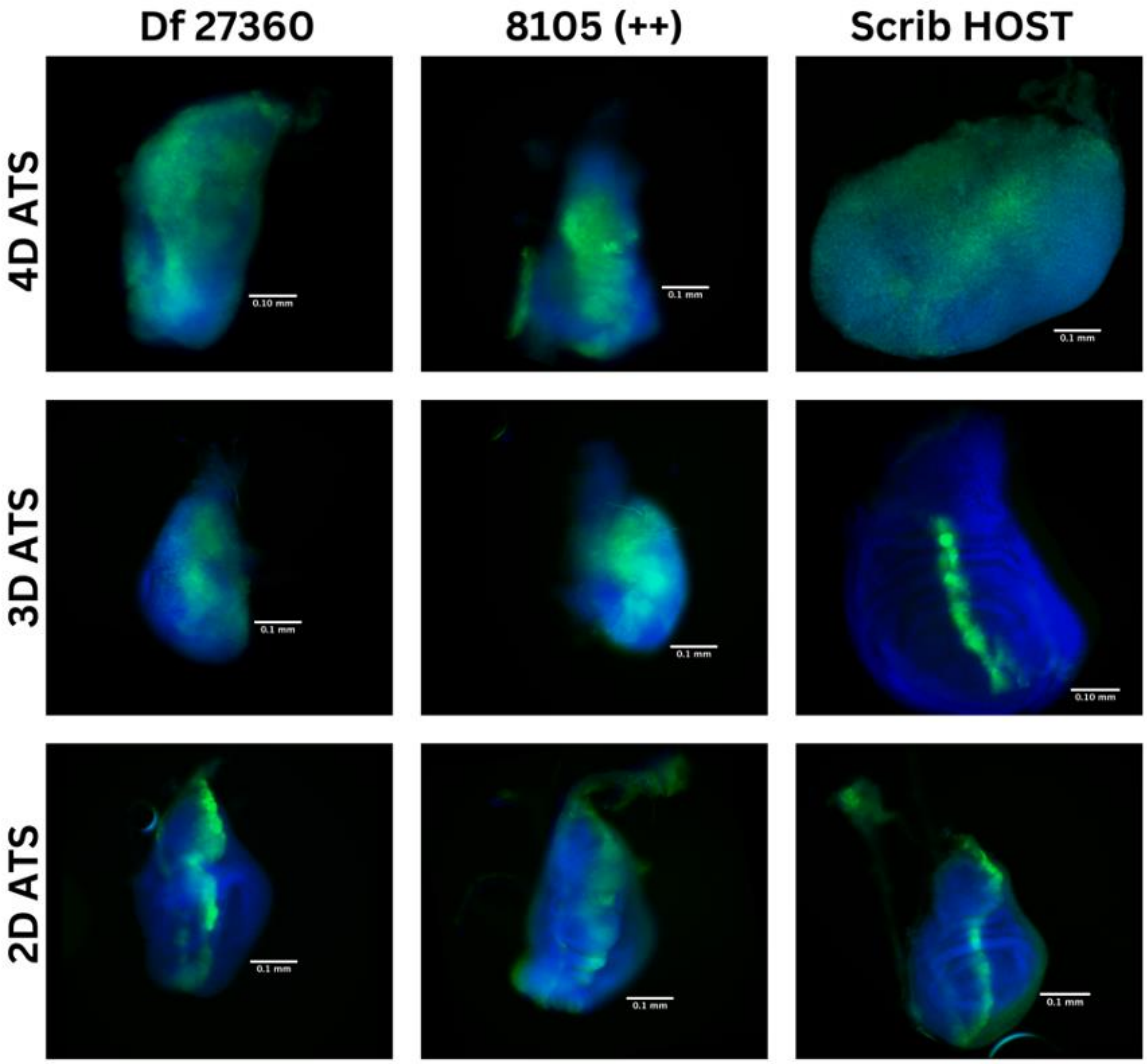

Figure 16. The influence of different time KD inductions on the wing disc tissue architecture. The first column represents Df line 27360. The positive-positive (++) and positive (+) control are shown in the second and third columns. The discs were stained with DAPI (blue) with GFP expression (green). A merged image of GFP and DAPI is created with ImageJ. The time inductions used: 2D ATS/3D ATS and 4DATS. Scale bar: 0.1 mm.

Hence, the time induction of the *scrib* KD is affecting the tissue architecture of the wing imaginal disc in a gradual manner. The deficiency line of our interest exhibits a strong loss of polarity phenotype and overgrowth of the discs. The phenotype of Df 27360 is consistent throughout the experiments, and the genetic interactions of *scrib* and the Df line are anticipated to occur.

3.2.7 The staining results of crucial cell polarity components

To examine the regulation of cell-cell adhesion, indicating the crucial factor of tissue integrity and tissue homeostasis, DE-Cadherin staining was conducted. (Wang et al., 2004) The experimental results are shown in the Figure 17.

The Df line 27360 and positive-positive (++) control exhibit uncontrolled proliferation and formation of neoplastic structures. The GFP stripe of *scrib* KD cells has expanded through the tissue structure. According to these results, the De-Cadherin was lost in the wing discs of all lines. The lack of De-Cadherin promotes cells to Epithelial-Mesenchymal Transition (EMT) and results in loss of epithelial structure of the cells. In contrast to Df line and positive-positive (++) control, positive (+) control did not exhibit such a strong phenotype, however the De-Cadherin is lost and the GFP stripe is expanded, implying the loss of polarity events occurred.

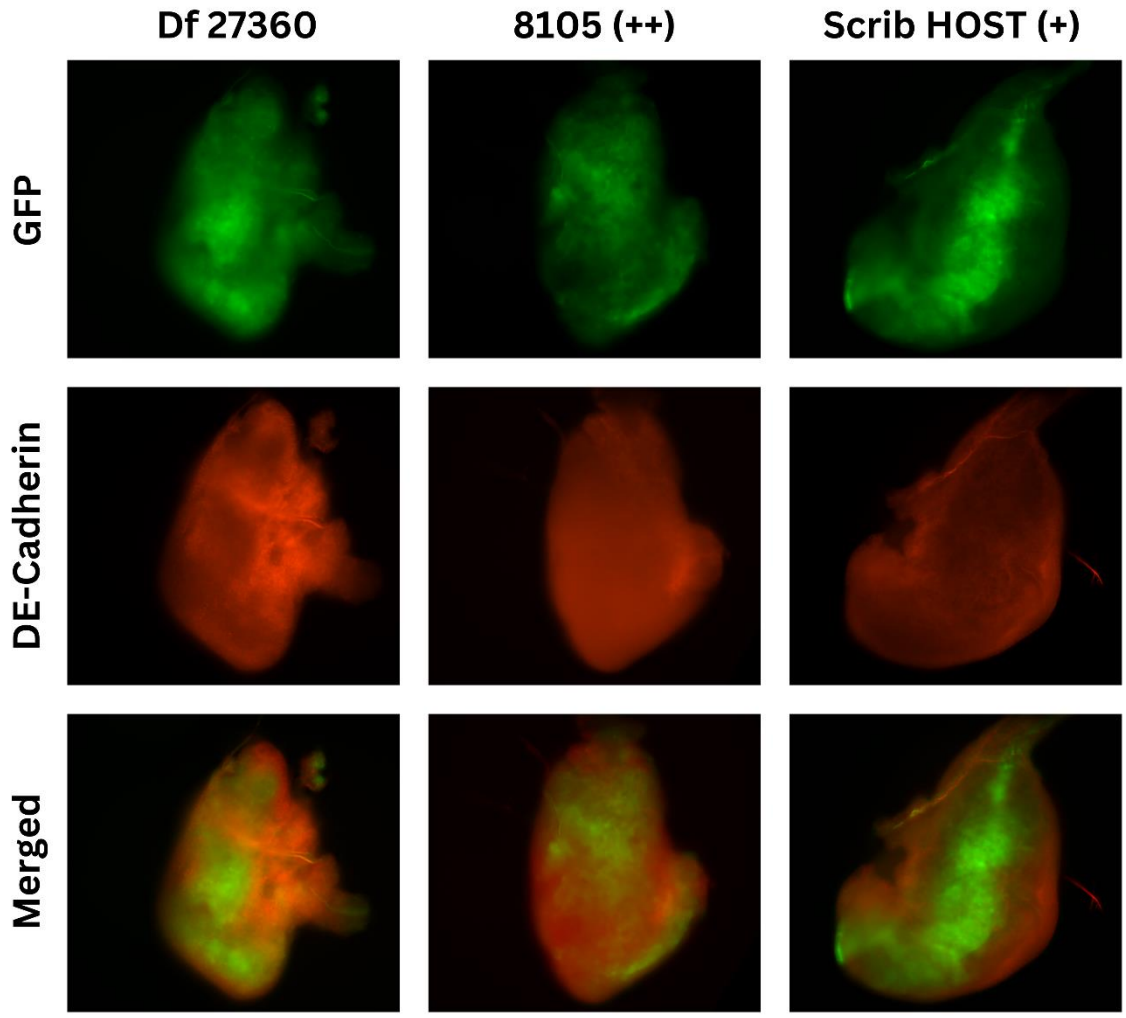

Figure 17. The DE-Cadherin expression in the wing disc of Df line 27360. The first column represents Df line 27360. The positive-positive (++) and positive (+) control are shown in the second and third columns. The discs were stained with DCAD2 (primary antibody, reddish colour) with GFP expression (green). A merged image of GFP and DCAD2 is created with ImageJ. The time inductions used: 3D ATS. Scale bar: 0.1 mm.

3.3 DISCUSSION

3.3.1 Results analysis and prospects for the future work

scrib KD leads to loss of polarity of the affected cells (Gui et al., 2021). The disruption of the polarity determinant leads to gradual depletion of the ABP within the tissue with the prolonged *scrib* RNAi KD. Previous work has shown that *scrib* interacts with several components of the epithelial cells to sustain the tissue homeostasis. (Huang et al., 2023).

In this thesis project, the potential novel genetic component of *scrib*-mediated tissue homeostasis was explored. The Df line 27360 screening experiments consistently demonstrated a phenotype characterized by overgrowth and disruption of the tissue architecture. Ex-LacZ was expressed at high levels within the tissue, showing the translocation of Yki into nucleus, subsequent hyperactivation of Yki and alteration of the Hippos signalling pathway.

Consequently, it appears important to investigate the particular gene, affecting the intercellular ABP maintenance, mechanism of the possible genetic interactions of *scrib* and the narrowed genomic region of Df line 27360.

3.3.1.1 The enhancement of the crossing protocol

In the attached results of the Df line 27360 secondary screening (Figure 17), *scrib* positive (+) control shows intense cell proliferation and neoplasia formation. Two primary factors can contribute to the following phenotype. The loss of TM6TBSB balancer could lead to appearance of the homozygous RNAi KD flies, which could possibly experience the double dosage of the mRNA degradation and, therefore, a more severe tumorigenic phenotype. Additionally, the *scrib* RNAi KD cells start to expand within the tissue from 2D ATS. (Gui et al., 2021), whereas in some experiments, the 3D ATS conditions were used in order to better visualise the difference between the positive-positive (++) control and Df line. However, this could affect the phenotype of the positive (+) control and further tests of the optimal protocol should be tested. For instance, 3.5D/2.5D ATS could be carried out. Due to the altering positive control phenotype in the Figure 15, it is essential to perform the experiment again with enhanced methodology.

To avoid the overexpression of the RNAi KD, the following crossing scheme of *scrib* RNAi host stock with the Df line could be proposed:

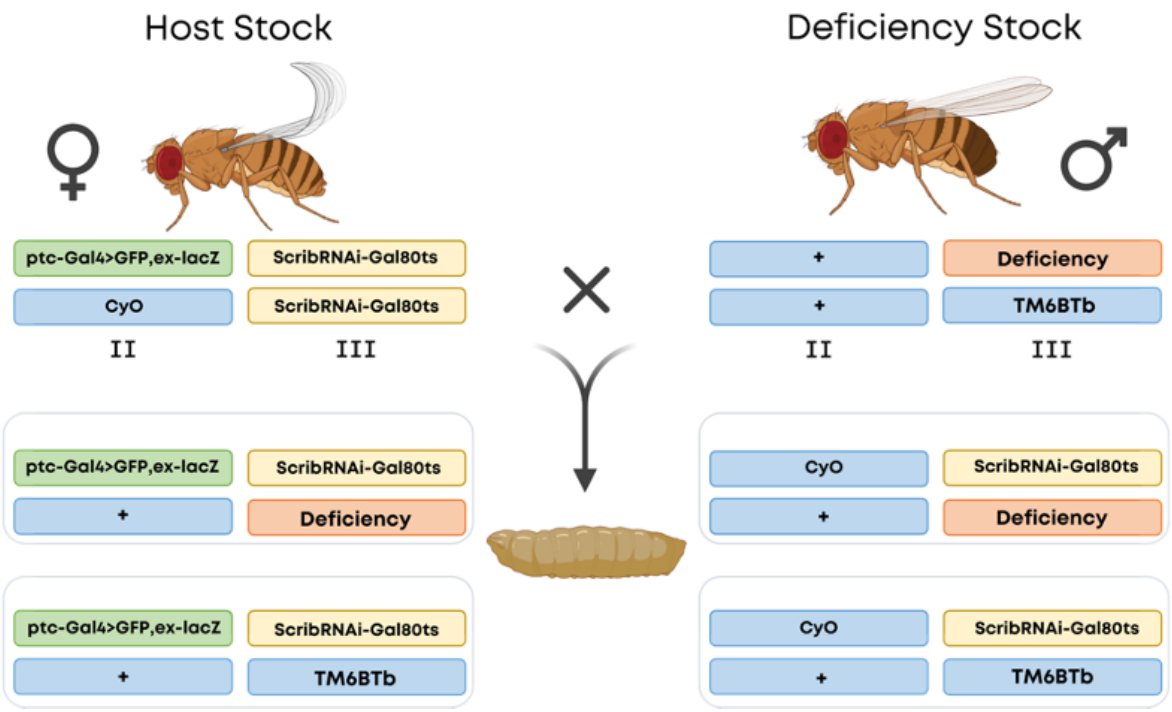

Figure 17. The logic of the cross with Df line with homozygous *scrib* RNAi KD stock.

Based on the scheme, the cross progeny received can be employed not only for the Df line balancer replacement but also to create controls, where the Df line of our interest can be replaced with 8105 positive-positive (++) control and to create a new stock of positive (+) control, with *scrib* RNAi KD and TM6TBSB. By following this scheme, the screening protocol can be enhanced.

3.3.1.2 Further investigation of specific gene alleles

The gene map of the strongest Df line candidate, the line of 27360, composed of 10 genes. The following table depicts all genes, found to be deleted in the region of Df 27360.

Table 3. The list of candidate genes.

Df line 27360 deleted genes names (BDSC)	
1.	*msi*
2.	*CG5107*
3.	*CG5111*
4.	*CG5112*
5.	*CG5116*
6.	*CG33494*
7.	*CG42488*
8.	*CG4553*
9.	*XNP*
10.	*Gnpat*

The current understanding of the functions of these genes in tumorigenesis and their interplay with *scrib* in mediating intercellular coordination of ABP is limited. Therefore, the subsequent feasible approach could be to explore the precise gene and the possible functions in the tissue homeostasis process, by conducting the screening experiments of the Df lines containing specific alleles of the mentioned genes.

3.3.2 The staining results of crucial cell polarity components

To examine the regulation of cell-cell adhesion, indicating the crucial factor of tissue integrity and tissue homeostasis, DE-Cadherin staining was conducted. (Wang et al., 2004) The experimental results are shown in the Figure 17.

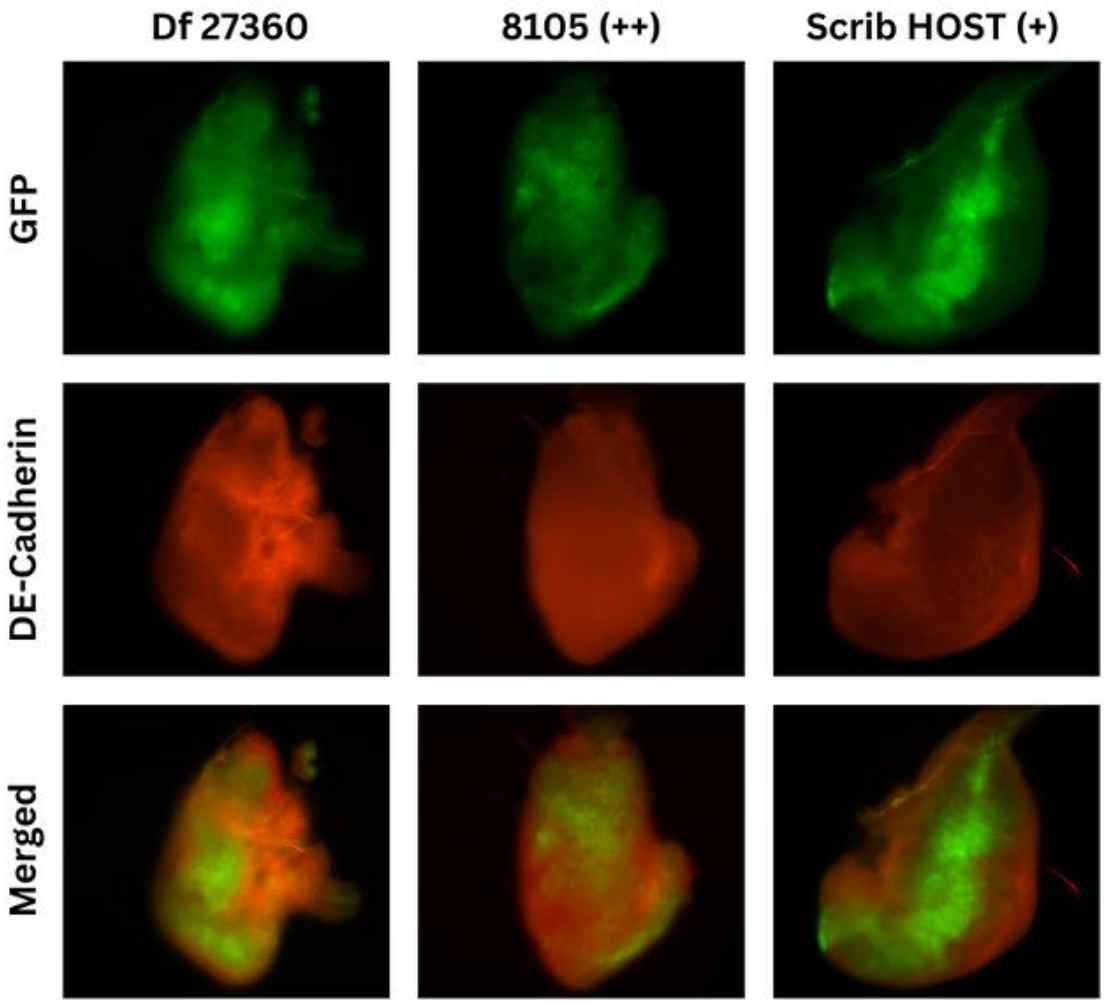

Figure 17. The DE-Cadherin expression in the wing disc of Df line 27360. The first column represents Df line 27360. The positive-positive (++) and positive (+) control are shown in the second and third columns. The discs were stained with DCAD2 (primary antibody, reddish colour) with GFP expression (green). A merged image of GFP and DCAD2 is created with ImageJ. The time inductions used: 3D ATS. Scale bar: 0.1 mm.

The Df line 27360 and positive-positive (++) control exhibit uncontrolled proliferation and formation of neoplastic structures. The GFP stripe of *scrib* KD cells has expanded through the tissue structure. According to these results, the De-Cadherin was lost in the wing discs of all lines. The lack of De-Cadherin promotes cells to Epithelial-Mesenchymal Transition (EMT) and results in loss of epithelial structure of the cells. In contrast to Df line and positive-positive (++) control, positive (+) control did not exhibit such a strong phenotype, however the De-Cadherin is lost and the GFP stripe is expanded, implying the loss of polarity events occurred.

SUMMARY

scrib is one of the key components in ABP establishment and a factor in tissue homeostasis. By introducing *scrib* RNAi KD in the group of cells, the progressing loss of polarity in the target and adjacent cell populations was observed. The interactions between *scrib*-RNAi KD and WT cells reveal the role of *scrib* in establishing intercellular alignment. Scrib interacts with α-Cat and SJs to relay the ABP signal in the neighbouring cells.

During this study, the possible Scrib-involved molecular network mechanisms were explored by the image-based screening in the fruit fly's specific genomic regions (deficiency lines) in the wing imaginal disc. The novel genetic candidate was found according to the stated research question:

- Which potential genes on the right arm of the third chromosome could contribute to regulating tissue homeostasis by maintaining ABP by having synergy with scribble?
- The candidate gene region, Df line 27360, was identified. The genomic region of the line contains ten genes, which may contribute to controlling tissue homeostasis by maintaining ABP by having synergetic interactions with the tumour suppressor gene, *scrib*.

REFERENCES

Adams, M. R., Celniker, S. E., Holt, R. J., Evans, C., Gocayne, J. D., Amanatides, P., Scherer, S. W., Li, P. R., Hoskins, R. A., Galle, R., George, R., Lewis, S. R., Richards, S., Ashburner, M., Henderson, S. N., Sutton, G. C., Wortman, J. R., Yandell, M., Zhang, Q., . . . Venter, J. C. (2000). The Genome Sequence of *Drosophila melanogaster*. *Science*, *287*(5461), 2185–2195. https://doi.org/10.1126/science.287.5461.2185

Aegerter-Wilmsen, T., Aegerter, C. M., Hafen, E., & Basler, K. (2007). Model for the regulation of size in the wing imaginal disc of Drosophila. *Mechanisms of Development*, *124*(4), 318–326. https://doi.org/10.1016/j.mod.2006.12.005

Aldaz, S., Escudero, L. M., & Freeman, M. C. (2010). Live imaging of *Drosophila* imaginal disc development. *Proceedings of the National Academy of Sciences of the United States of America*, *107*(32), 14217–14222. https://doi.org/10.1073/pnas.1008623107

Allocca, M., Zola, S., & Bellosta, P. (2018). The Fruit Fly, Drosophila melanogaster: The Making of a Model (Part I). In *InTech eBooks*. InTech. https://doi.org/10.5772/intechopen.72832

Baumgartner, S. V., Littleton, J. T., Broadie, K., Bhat, M. A., Harbecke, R., Lengyel, J. A., Chiquet-Ehrismann, R., Prokop, A., & Bellen, H. J. (1996). A Drosophila Neurexin Is Required for Septate Junction and Blood-Nerve Barrier Formation and Function. *Cell*, *87*(6), 1059–1068. https://doi.org/10.1016/s0092-8674(00)81800-0

Beira, J. V., & Paro, R. (2016). The legacy of Drosophila imaginal discs. *Chromosoma*, *125*(4), 573–592. https://doi.org/10.1007/s00412-016-0595-4

Benson, K. R. (2001). T. H. Morgan's resistance to the chromosome theory. *Nature Reviews Genetics*, *2*(6), 469–474. https://doi.org/10.1038/35076532

Bilder, D. (2004). Epithelial polarity and proliferation control: links from the *Drosophila* neoplastic tumor suppressors. *Genes & Development*, *18*(16), 1909–1925. https://doi.org/10.1101/gad.1211604

Bilder, D., Minteer, S. D., & Perrimon, N. (2000). Cooperative Regulation of Cell Polarity and Growth by *Drosophila* Tumor Suppressors. *Science*, *289*(5476), 113–116. https://doi.org/10.1126/science.289.5476.113

Blake, A. J., Finger, D. S., Hardy, V. L., & Ables, E. T. (2017). RNAi-Based Techniques for the Analysis of Gene Function in Drosophila Germline Stem Cells. In *Methods in molecular biology* (pp. 161–184). Springer Science+Business Media. https://doi.org/10.1007/978-1-4939-7108-4_13

Bonello, T. T., Choi, W., & Peifer, M. (2019). scribble and discs-large direct initial assembly and positioning of adherens junctions during establishment of apical-basal polarity. *Development*. https://doi.org/10.1242/dev.180976

Bowling, S., Lawlor, K., & Rodriguez, T. A. (2019). Cell competition: the winners and losers of fitness selection. *Development*, *146*(13). https://doi.org/10.1242/dev.167486

Brand, A. H., & Perrimon, N. (1993). Targeted gene expression as a means of altering cell fates and generating dominant phenotypes. *Development*, *118*(2), 401–415. https://doi.org/10.1242/dev.118.2.401

Brumby, A. M., & Richardson, H. E. (2003a). scribble mutants cooperate with oncogenic Ras or Notch to cause neoplastic overgrowth in Drosophila. *The EMBO Journal*, *22*(21), 5769–5779. https://doi.org/10.1093/emboj/cdg548

Carmena, A. (2020). The Case of the scribble Polarity Module in Asymmetric Neuroblast Division in Development and Tumorigenesis. *International Journal of Molecular Sciences*, *21*(8), 2865. https://doi.org/10.3390/ijms21082865

Chen, C., Schroeder, M. C., Kango-Singh, M., Tao, C., & Halder, G. (2012). Tumor suppression by cell competition through regulation of the Hippo pathway. *Proceedings of the National Academy of Sciences*, *109*(2), 484–489. https://doi.org/10.1073/pnas.1113882109

Chen, Y., Han, H., Seo, G., Vargas, R., Yang, B., Chuc, K., Zhao, H., & Wang, W. (2020). Systematic analysis of the Hippo pathway organization and oncogenic alteration in evolution. *Scientific Reports*, *10*(1). https://doi.org/10.1038/s41598-020-60120-4

De La Cova, C., Abril, M., Bellosta, P., Gallant, P., & Johnston, L. (2004). Drosophila Myc Regulates Organ Size by Inducing Cell Competition. *Cell*, *117*(1), 107–116. https://doi.org/10.1016/s0092-8674(04)00214-4

Doggett, K., Grusche, F. A., Richardson, H. E., & Brumby, A. M. (2011). Loss of the Drosophila cell polarity regulator *scrib*bled promotes epithelial tissue overgrowth and cooperation with oncogenic Ras-Raf through impaired Hippo pathway signaling. *BMC Developmental Biology*, *11*(1). https://doi.org/10.1186/1471-213x-11-57

Dong, J., Feldmann, G., Huang, J., Wu, S., Zhang, N., Comerford, S. A., Gayyed, M. F., Anders, R. A., Maitra, A., & Pan, D. (2007). Elucidation of a Universal Size-Control Mechanism in Drosophila and Mammals. *Cell*, *130*(6), 1120–1133. https://doi.org/10.1016/j.cell.2007.07.019

Drubin, D. G., & Nelson, W. J. (1996). Origins of Cell Polarity. *Cell*, *84*(3), 335–344. https://doi.org/10.1016/s0092-8674(00)81278-7

Duffy, J. R. (2002). GAL4 system indrosophila: A fly geneticist's swiss army knife. *Genesis*, *34*(1–2), 1–15. https://doi.org/10.1002/gene.10150

Dye, N. A., Popović, M., Spannl, S., Etournay, R., Kainmüller, D., Ghosh, S., Myers, E. N., Jülicher, F., & Eaton, S. (2017). Cell dynamics underlying oriented growth of the-*Drosophila*wing imaginal disc. *Development*. https://doi.org/10.1242/dev.155069

Edgar, B. A. (2006). How flies get their size: genetics meets physiology. *Nature Reviews Genetics*, *7*(12), 907–916. https://doi.org/10.1038/nrg1989

Enomoto, M., & Igaki, T. (2022). Cell-cell interactions that drive tumorigenesis in *Drosophila*. *Fly*, *16*(1), 367–381. https://doi.org/10.1080/19336934.2022.2148828

Enomoto, M., Takemoto, D., & Igaki, T. (2021). Interaction between Ras and Src clones causes interdependent tumor malignancy via Notch signaling in Drosophila. *Developmental Cell*, *56*(15), 2223-2236.e5. https://doi.org/10.1016/j.devcel.2021.07.002

Everetts, N. J., Worley, M. I., Yasutomi, R., Yosef, N., & Hariharan, I. K. (2021). Single-cell transcriptomics of the Drosophila wing disc reveals instructive epithelium-to-myoblast interactions. *eLife*, *10*. https://doi.org/10.7554/elife.61276

FlyBase. (n.d.). *FlyBase Homepage*. https://flybase.org/

Fuse, N., Hirose, S., & Hayashi, S. (1996). Determination of wing cell fate by the escargot and snail genes in Drosophila. *Development*, *122*(4), 1059–1067. https://doi.org/10.1242/dev.122.4.1059

Gibson, M. I., & Perrimon, N. (2003). Apicobasal polarization: epithelial form and function. *Current Opinion in Cell Biology*, *15*(6), 747–752. https://doi.org/10.1016/j.ceb.2003.10.008

Gilbert, S. F. (2000). Early Drosophila Development. In *Developmental Biology - NCBI Bookshelf*. https://www.ncbi.nlm.nih.gov/books/NBK10081/

Gui, J., Huang, Y., Montanari, M. P., Toddie-Moore, D., Kikushima, K., Nix, S., Ishimoto, Y., & Shimmi, O. (2019). Coupling between dynamic 3D tissue architecture and BMP morphogen signaling during *Drosophila* wing morphogenesis. *Proceedings of the National Academy of Sciences of the United States of America*, *116*(10), 4352–4361. https://doi.org/10.1073/pnas.1815427116

Halder, G., & Johnson, R. L. (2011). Hippo signaling: growth control and beyond. *Development*, *138*(1), 9–22. https://doi.org/10.1242/dev.045500

Hales, K. H., Korey, C. A., Larracuente, A. M., & Roberts, D. D. (2015a). Genetics on the Fly: A Primer on the *Drosophila* Model System. *Genetics*, *201*(3), 815–842. https://doi.org/10.1534/genetics.115.183392

Halpern, M. E., Rhee, J. M., Goll, M. G., Akitake, C. M., Parsons, M. T., & Leach, S. D. (2008). Gal4/UAS Transgenic Tools and Their Application to Zebrafish. *Zebrafish*, *5*(2), 97–110. https://doi.org/10.1089/zeb.2008.0530

Harden, N., Wang, S., & Krieger, C. (2016). Making the connection – shared molecular machinery and evolutionary links underlie the formation and plasticity of occluding junctions and synapses. *Journal of Cell Science*, *129*(16), 3067–3076. https://doi.org/10.1242/jcs.186627

Heigwer, F., Port, F., & Boutros, M. (2018). RNA Interference (RNAi) Screening in Drosophila. Genetics, 208(3), 853–874. https://doi.org/10.1534/genetics.117.300077

Huang, Y., Gui, J., Myllymäki, S., Mikkola, M. L., & Shimmi, O. (2023). Coordination of tissue homeostasis and growth by the scribble-α-Catenin-Septate junction complex. *iScience*, *26*(4), 106490. https://doi.org/10.1016/j.isci.2023.106490

Huang, Y., Gui, J., Myllymäki, S., Roy, K. K., Tõnissoo, T., Mikkola, M. L., & Shimmi, O. (2022). scribble and α-Catenin cooperatively regulate epithelial homeostasis and growth. *Frontiers in Cell and Developmental Biology*, *10*. https://doi.org/10.3389/fcell.2022.912001

Igaki, T., Pagliarini, R., & Xu, T. (2006). Loss of Cell Polarity Drives Tumor Growth and Invasion through JNK Activation in Drosophila. *Current Biology*, *16*(11), 1139–1146. https://doi.org/10.1016/j.cub.2006.04.042

Jabbarzadeh, E. (2019). Polarity as a physiological modulator of cell function. *Frontiers in Bioscience*, *24*(3), 451–462. https://doi.org/10.2741/4728

Jaiswal, M., Agrawal, N., & Sinha, P. (2006). Fat and Wingless signaling oppositely regulate epithelial cell-cell adhesion and distal wing development in*Drosophila*. *Development*, *133*(5), 925–935. https://doi.org/10.1242/dev.02243

Jennings, B. A. (2011). Drosophila – a versatile model in biology & medicine. *Materials Today*, *14*(5), 190–195. https://doi.org/10.1016/s1369-7021(11)70113-4

Kanda, H., & Igaki, T. (2020a). Mechanism of tumor-suppressive cell competition in flies. *Cancer Science*, *111*(10), 3409–3415. https://doi.org/10.1111/cas.14575

Karaman, R., & Halder, G. (2018). Cell Junctions in Hippo Signaling. *Cold Spring Harbor Perspectives in Biology*, *10*(5), a028753. https://doi.org/10.1101/cshperspect.a028753

Kaufman, T. C. (2017). A Short History and Description of *Drosophila melanogaster* Classical Genetics: Chromosome Aberrations, Forward Genetic Screens, and the Nature of Mutations. *Genetics*, *206*(2), 665–689. https://doi.org/10.1534/genetics.117.199950

Khoury, M. J., & Bilder, D. (2020). Distinct activities of *scrib* module proteins organize epithelial polarity. *Proceedings of the National Academy of Sciences of the United*

States of America, *117*(21), 11531–11540. https://doi.org/10.1073/pnas.1918462117

Khursheed, M., & Bashyam, M. D. (2014). Apico-basal polarity complex and cancer. *Journal of Biosciences*, *39*(1), 145–155. https://doi.org/10.1007/s12038-013-9410-z

Klein, T. W. (2001). Wing disc development in the fly: the early stages. *Current Opinion in Genetics & Development*, *11*(4), 470–475. https://doi.org/10.1016/s0959-437x(00)00219-7

Lee, M., & Vasioukhin, V. (2008). Cell polarity and cancer – cell and tissue polarity as a non-canonical tumor suppressor. *Journal of Cell Science*, *121*(8), 1141–1150. https://doi.org/10.1242/jcs.016634

Llorens-Giralt, P., Camilleri-Robles, C., Corominas, M., & Climent-Cantó, P. (2021). Chromatin Organization and Function in Drosophila. *Cells*, *10*(9), 2362. https://doi.org/10.3390/cells10092362

Macara, I. G. (2004). Parsing the Polarity Code. *Nature Reviews Molecular Cell Biology*, *5*(3), 220–231. https://doi.org/10.1038/nrm1332

McClure, K. D., & Schubiger, G. (2005). Developmental analysis and squamous morphogenesis of the peripodial epithelium in Drosophila imaginal discs. *Development*, *132*(22), 5033–5042. https://doi.org/10.1242/dev.02092

Mirzoyan, Z., Sollazzo, M., Allocca, M., Valenza, A., Grifoni, D., & Bellosta, P. (2019). Drosophila melanogaster: A Model Organism to Study Cancer. *Frontiers in Genetics*, *10*, 51. https://doi.org/10.3389/fgene.2019.00051

Moreno, E., & Basler, K. (2004). dMyc Transforms Cells into Super-Competitors. *Cell*, *117*(1), 117–129. https://doi.org/10.1016/s0092-8674(04)00262-4

Ohsawa, S., Sato, Y., Enomoto, M., Nakamura, M., Betsumiya, A., & Igaki, T. (2012). Mitochondrial defect drives non-autonomous tumour progression through Hippo signalling in Drosophila. *Nature*, *490*(7421), 547–551. https://doi.org/10.1038/nature11452

Ong, C. N., Yung, L. L., Cai, Y., Bay, B., & Baeg, G. H. (2015). *Drosophila melanogaster*as a model organism to study nanotoxicity. *Nanotoxicology*, *9*(3), 396–403. https://doi.org/10.3109/17435390.2014.940405

Ostalé, C. M., Ruiz-Gómez, A., Vega, P., Losada, M., Estella, C., & De Celis, J. F. (2018). Drosophila Imaginal Discs as a Playground for Genetic Analysis: Concepts, Techniques and Expectations for Biomedical Research. In *InTech eBooks*. InTech. https://doi.org/10.5772/intechopen.72758

Pagliarini, R., & Xu, T. (2003). A Genetic Screen in *Drosophila* for Metastatic Behavior. *Science*, *302*(5648), 1227–1231. https://doi.org/10.1126/science.1088474

Perveen, F. (2018). Introduction to Drosophila. *InTech eBooks*. https://doi.org/10.5772/67731

Porter, R., & Rivers, J. (1975). Ciba Foundation Symposium 29 - Cell Patterning. In *Novartis Foundation Symposium*. Wiley. https://doi.org/10.1002/9780470720110

Qin, Y., Capaldo, C. T., Gumbiner, B. M., & Macara, I. G. (2005). The mammalian scribble polarity protein regulates epithelial cell adhesion and migration through E-cadherin. *Journal of Cell Biology*, *171*(6), 1061–1071. https://doi.org/10.1083/jcb.200506094

Requena, D., Álvarez, J., Gabilondo, H., Loker, R., Mann, R. S., & Estella, C. (2017). Origins and Specification of the Drosophila Wing. *Current Biology*, *27*(24), 3826-3836.e5. https://doi.org/10.1016/j.cub.2017.11.023

Rübsam, M., Mertz, A. F., Kubo, A., Marg, S., Jüngst, C., Goranci-Buzhala, G., Schauss, A., Horsley, V., Dufresne, E. R., Moser, M., Ziegler, W., Amagai, M., Wickström, S. A., & Niessen, C. M. (2017). E-cadherin integrates mechanotransduction and EGFR signaling to control junctional tissue polarization and tight junction positioning. *Nature Communications*, *8*(1). https://doi.org/10.1038/s41467-017-01170-7

Rudrapatna, V. A., Cagan, R. L., & Das, T. P. (2012). *Drosophila Cancer* models. *Developmental Dynamics*, *241*(1), 107–118. https://doi.org/10.1002/dvdy.22771

Shingleton, A. W. (2010). The regulation of organ size in Drosophila. In *Organogenesis* (Vol. 6, Issue 2, pp. 76–87). Taylor & Francis. https://doi.org/10.4161/org.6.2.10375

Tepass, U., & Harris, K. A. (2007). Adherens junctions in Drosophila retinal morphogenesis. *Trends in Cell Biology*, *17*(1), 26–35. https://doi.org/10.1016/j.tcb.2006.11.006

Tepass, U., Theres, C., & Knust, E. (1990). crumbs encodes an EGF-like protein expressed on apical membranes of Drosophila epithelial cells and required for organization of epithelia. *Cell*, *61*(5), 787–799. https://doi.org/10.1016/0092-8674(90)90189-l

Thompson, B. C. (2013). Cell polarity: models and mechanisms from yeast, worms and flies. *Development*, *140*(1), 13–21. https://doi.org/10.1242/dev.083634

Tolwinski, N. S. (2017). Introduction: Drosophila—A Model System for Developmental Biology. *Journal of Developmental Biology*, *5*(3), 9. https://doi.org/10.3390/jdb5030009

Tripathi, B. K., & Irvine, K. (2022). The wing imaginal disc. *Genetics*, *220*(4). https://doi.org/10.1093/genetics/iyac020

Wang, F., Dumstrei, K., Haag, T. W., & Hartenstein, V. (2004). The role of DE-cadherin during cellularization, germ layer formation and early neurogenesis in the Drosophila embryo. *Developmental Biology*, *270*(2), 350–363. https://doi.org/10.1016/j.ydbio.2004.03.002

Woods, D. F., Hough, C., Peel, D., Callaini, G., & Bryant, P. (1996). Dlg protein is required for junction structure, cell polarity, and proliferation control in Drosophila epithelia. *Journal of Cell Biology*, *134*(6), 1469–1482. https://doi.org/10.1083/jcb.134.6.1469

Vaccari, T., & Bilder, D. (2005). The Drosophila Tumor Suppressor vps25 Prevents Nonautonomous Overproliferation by Regulating Notch Trafficking. *Developmental Cell*, *9*(5), 687–698. https://doi.org/10.1016/j.devcel.2005.09.019

Yu, F., & Guan, K. (2013). The Hippo pathway: regulators and regulations. *Genes & Development*, *27*(4), 355–371. https://doi.org/10.1101/gad.210773.112

Yu, J., & Pan, D. (2018). Validating upstream regulators of Yorkie activity in Hippo signaling through *scalloped*-based genetic epistasis. *Development*, *145*(4). https://doi.org/10.1242/dev.157545

Zhao, B., Wei, X., Li, W., Udan, R. S., Yang, Q., Kim, J., Xie, J. X., Ikenoue, T., Yu, J., Li, L., Zhang, P., Ye, K., Chinnaiyan, A. M., Halder, G., Lai, Z. C., & Guan, K. (2007). Inactivation of YAP oncoprotein by the Hippo pathway is involved in cell contact inhibition and tissue growth control. *Genes & Development*, *21*(21), 2747–2761. https://doi.org/10.1101/gad.1602907

Zheng, Y., & Pan, D. (2019a). The Hippo Signaling Pathway in Development and Disease. *Developmental Cell*, *50*(3), 264–282. https://doi.org/10.1016/j.devcel.2019.06.003

Zeitler, J., Hsu, C., Dionne, H., & Bilder, D. (2004c). Domains controlling cell polarity and proliferation in the Drosophila tumor suppressor scribble. *Journal of Cell Biology*, *167*(6), 1137–1146. https://doi.org/10.1083/jcb.200407158

NON-EXCLUSIVE LICENCE TO REPRODUCE THESIS AND MAKE THESIS PUBLIC

I, Eva Savulkina,

1. herewith grant the University of Tartu a free permit (non-exclusive licence) to

reproduce, for the purpose of preservation, including for adding to the DSpace digital archives until the expiry of the term of copyright,

Investigating gene synergistic interactions: Screening for novel components of intercellular alignment in Drosophila wing disc epithelium,

supervised by Osamu Shimmi.

2. I grant the University of Tartu a permit to make the work specified in p. 1 available to the public via the web environment of the University of Tartu, including via the DSpace digital archives, under the Creative Commons licence CC BY NC ND 3.0, which allows, by giving appropriate credit to the author, to reproduce, distribute the work and communicate it to the public, and prohibits the creation of derivative works and any commercial use of the work until the expiry of the term of copyright.

3. I am aware of the fact that the author retains the rights specified in p. 1 and 2.

4. I certify that granting the non-exclusive licence does not infringe other persons' intellectual property rights or rights arising from the personal data protection legislation.

Eva Savulkina

24/05/2023